University of Minnesota
St. Anthony Falls Hydraulic Laboratory

Project Report No. 164

CALUMET PUMPING STATION
HYDRAULIC MODEL STUDY

by

Heinz Stefan

and

Addison Wood

Prepared for

DELEUW, CATHER AND COMPANY
Chicago, Illinois

May 1977
Minneapolis, Minnesota

CONTENTS

ABSTRACT AND SUMMARY

A hydraulic model of the underground pump suction intake structure of the Calumet Pumping Station was built and tested. The pumping station is an element of the projected Chicago storm runoff collection and treatment system, to be completed within the next few years. The study was conducted for DeLeuw, Cather and Co., Consulting Engineers and Planners, Chicago, Illinois, on behalf of the Metropolitan Sanitary District of Greater Chicago.

The model was built at a scale of 1:14, mostly out of plexiglass to facilitate observation. The model included the downstream end of the Calumet Tunnel, a drop structure, two symmetrically placed ducts, a wet shaft and a suction header with three branch pipes as shown in Figs. 1 through 8.

It was the objective of the hydraulic model study to identify and document (a) problems with flow separation, secondary currents and vortex formation by flow visualization, (b) air entrappment and air entrainment during filling and during pump operation, (c) piezometric heads and head losses throughout the structure, (d) accumulation and entrainment of fuel oil, resulting from accidental spills, throughout the structure (e) transport and deposition of grit throughout the structure.

As a result of the initial observations made in the model, the structure was modified in two locations to improve flow characteristics and to reduce grit deposition. The observations made in the model with regard to flow patterns, air entrainment and fuel entrainment have been documented by still pictures (black and white) and color motion picture. Head losses are reported in tabular and graphical form. The performance of the structure (Design C in Fig. 10) with respect to air entrainment, fuel entrainment and head losses appears quite satisfactory. Grit deposition was largely reduced but not fully eliminated.

The following specific findings and recommendations were made:

At high stages, that is at the beginning of the pumping cycle, flow through the structure is at low velocity and with little flow separation occurring. At low stages, flow in the drop structure becomes highly turbulent resulting at first in entrainment of floating materials and at W.S. stages below -320 in entrainment of air into the duct. In the wet shaft, there appears to be no tendency for vortex formation or air entrainment into the suction header. Only the complete blockage of the lower portion of the bar screen caused a vortex in the wet shaft.

It was recommended that three air vents be installed on the suction header at the intersection of each of the three branch pipe axis with the suction header wall. These vents will prevent air accumulation in the branch header during filling.

Head losses throughout the structure were found to be small. They are summarized on pages 47 and 48. Piezometric grade lines are shown in Figs. 46, 47, and 48.

A major grit deposition problem existed in the divided duct due to the large reduction in flow velocities and bed shear stresses in that part of the structure. A reduction in cross-sectional area by raising the invert by several feet resulted in a significant reduction in grit deposition. Complete elimination of grit deposition appears possible with further reductions of duct width.

List of Figures (Cont'd.)

INTRODUCTION

In order to reduce water pollution in Lake Michigan the Metropolitan Sanitary District of Greater Chicago is implementing plans for the collection, temporary storage, and treatment of storm water runoff from the downtown and suburban metropolitan area. To this end, an extensive system of underground tunnels will be built for collection and storage of stormwater. It will be necessary to pump the water to a treatment plant before discharge.

As part of this project, DeLeuw, Cather and Company, Consulting Engineers and Planners, Chicago, designed the Calumet Pumping Station as described in their Design Memorandum for Calumet Pumping Station, Contract 74-206-2h Calumet Tunnel System (86 pages and 10 plates), 1976. With the concurrence of the Sanitary District of Greater Chicago, the company requested the St. Anthony Falls Hydraulic Laboratory to study the inlet (suction) portion of the pumping station in a hydraulic model. The geometry of this part of the system is complicated and a number of questions have been asked which can only be answered by model experiments.

CALUMET PUMPING STATION DESIGN

The suction side of the Calumet Pumping Station connects the Calumet Tunnel to six pumps which are located in two fully symmetrical underground pump rooms. The system is geometrically complex and includes the following major elements:

(a) the 21' diameter Calumet tunnel

(b) a box drop inlet (drop structure)

(c) two symmetrically placed ducts

(d) two symmetrically placed separate wetshafts

(e) two symmetrically placed suction headers, each feeding a group of three pumps.

Appropriate transitions connect these various elements. A sectional, schematic view of the Calumet Pumping Station and the portion represented in the model is shown in Fig. 1. The preliminary design of the structural elements required is shown in more detail in the before-mentioned memorandum. Figs. 1, 2, and 3 are reproductions from that memorandum. Blueprints, which served as a basis for the model design were supplied by DeLeuw, Cather and Company.

The total design pumping rates of the station with two 600 rpm pumps and one 900 rpm pump in operation in each pump room are according to the before-mentioned memorandum as shown in Fig. 4. Low water wet shaft elevation is -322. Pump no. 1 with 50 cfs would be used to draw water levels below -322. It was agreed that experiments would concentrate on flows of 600 cfs, 400 cfs, 200 cfs and 50 cfs.

OBJECTIVE OF STUDY

In general, the design of the suction side of any pumping system requires critical evaluation with regard to potential occurrence of air entrainment or low pressures causing a cavitation potential inside the pump. Since the geometrical complexity of the suction side of the Calumet Pumping Station does not permit analysis, observations and measurements in a geometrically and dynamically similar hydraulic model are necessary. Specific objectives of the hydraulic model study undertaken were:

1. Flow visualization to identify flow patterns, separation zones, and secondary currents.
2. Determination and documentation (photography) of the susceptibility of the system to vortex formation and air entrainment in those portions of the system where a free water surface is present. Most critical would be the wet shaft area under very low stage and high

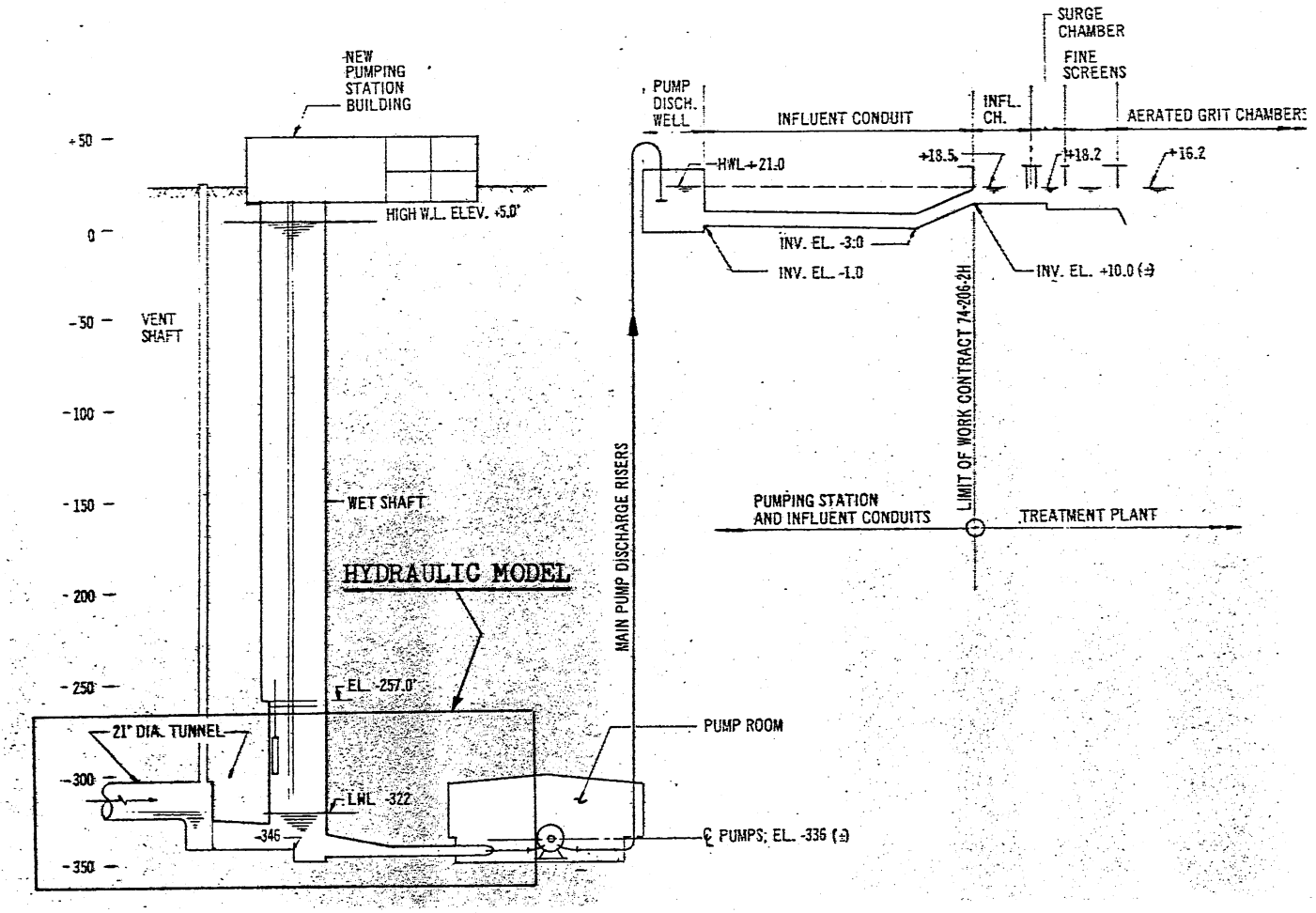

Fig. 1 - Preliminary Sectional View of Calumet Pumping Station

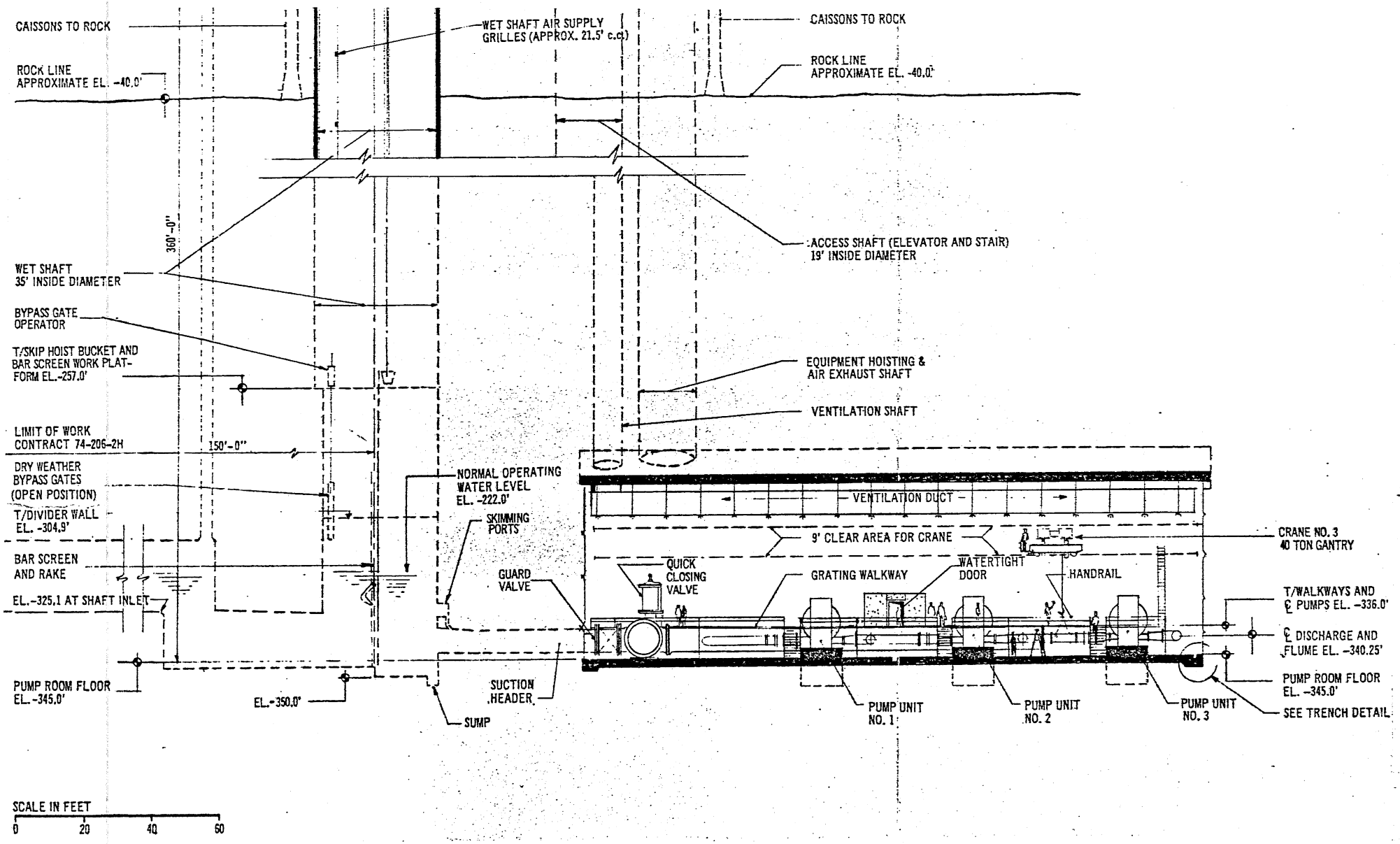

Fig. 2 - Longitudinal Section

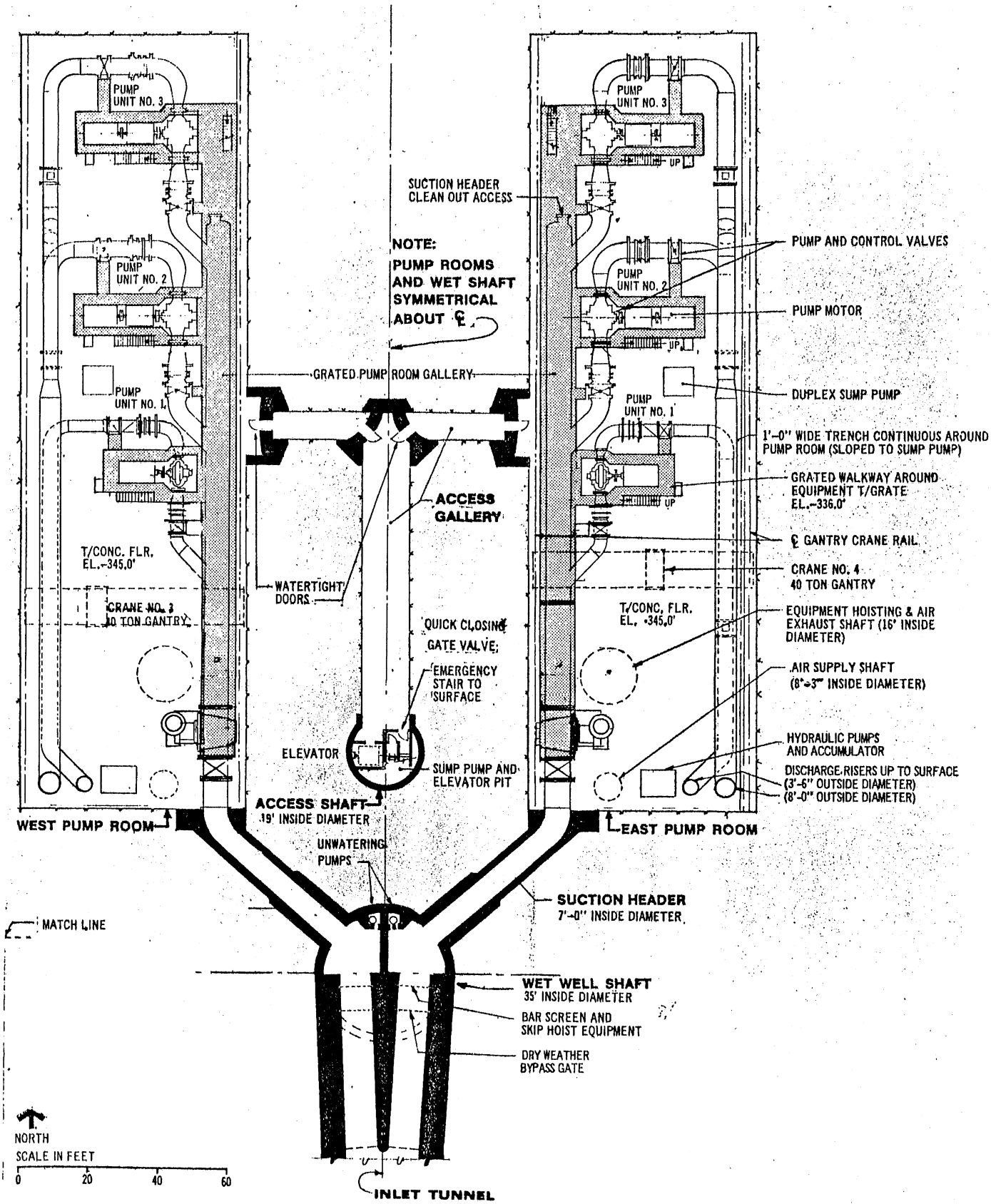

Fig. 3 - Pump Room Plan

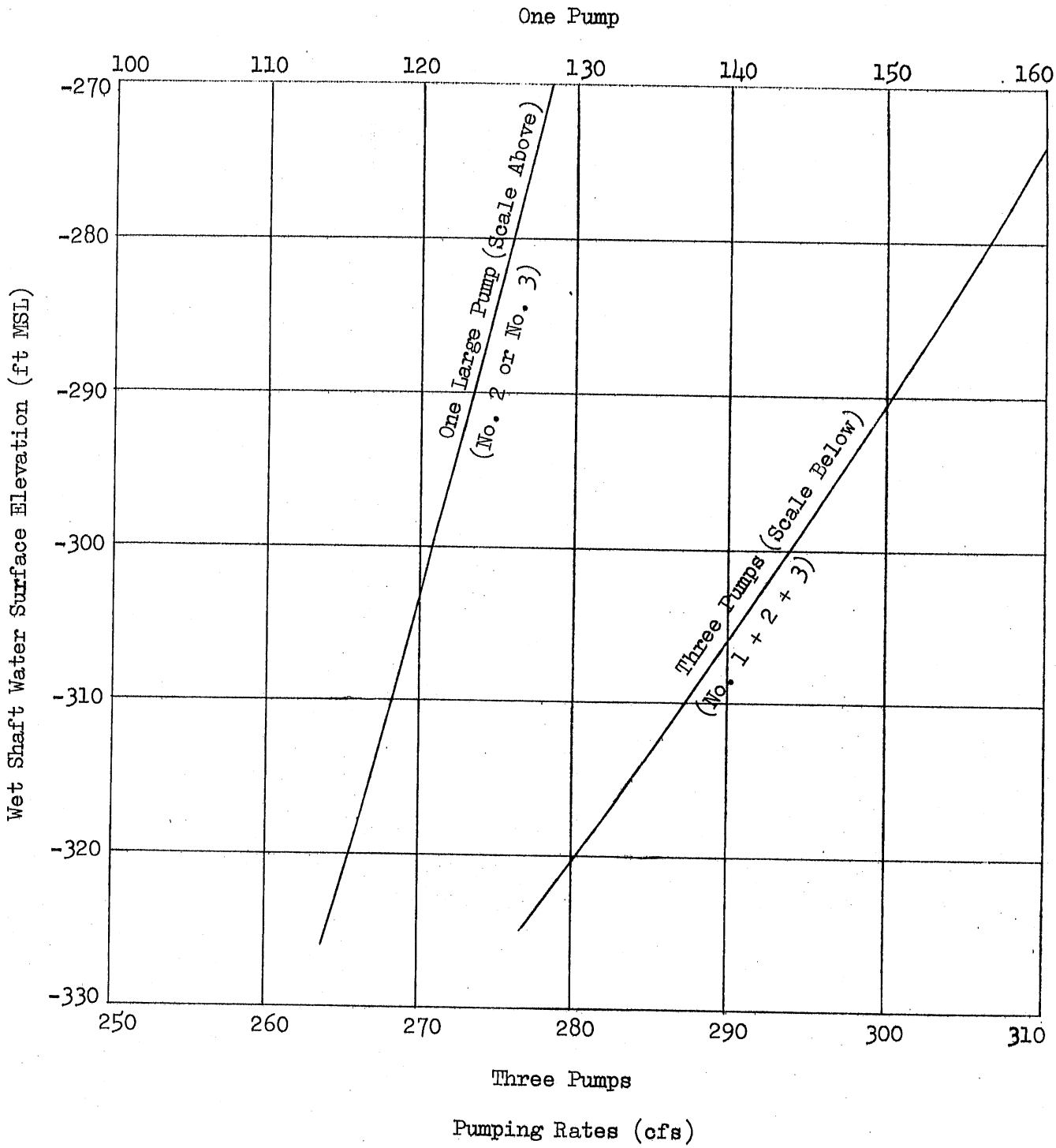

Fig. 4 - Head-Capacity Curves for Pumps

flow, i.e. at W.S. elevation -322 in the wet shaft and at a total flow rate of 600 cfs. Conditions at higher stages in the wet shaft were also considered for testing.

3. Observation of air entrappment in the suction header during the filling. Determination of optimum placement of air vents on the suction header.

4. Measurement of pressures at selected points and computation of head losses and loss coefficients for non-air entraining conditions.

5. Determination of the entrainment of floating materials particularly floating liquids such as fuel oil which could accumulate in the storm water collection system after accidental spills.

6. Observation and documentation of the transport and deposition of grit throughout the system.

SCALE MODEL DESIGN

The model was designed for a geometrical scale ratio of 1:14. This scale was chosen primarily to permit selection of commercially available pipe sizes for the suction header and the branch pipes. The model also had to be large enough to produce fully developed turbulent flow. Flow rates and velocities were most frequently scaled according to Froude similarity since gravity and/or inertial effects were dominant throughout major portions of the structure. This was adequate for the scaling of vortex formation, secondary currents and flow separation. The scaling of air entrainment and grit transport was only qualitative. For the study of head losses in the full flowing suction header, highest attainable Reynolds numbers were used in the model. Additional information on scaling is given in the Appendix.

For experiments using Froude similarity, prototype quantities were reduced by the following scale ratios:

Distances (lengths) and elevation (heights)	1:14.0
Flow velocities	1:3.74
Residence times	1:3.74
Flow rates	1:733.4
Pressures and pressure heads	1:14.0
Forces	1:2744.0

Some typical model dimensions were as follows:

Diameter of Calumet tunnel	18 inches
Diameter of main suction header	6 inches
Diameter of branch header to pump 1	3 inches
Diameter of branch header to pumps 2 and 3	4 inches

The diameter of the branch header to pumps 2 and 3 should have been 4.28 inches I.D. a size which is not commercially available. Measurements of pressures in that pipe as reported herein were adjusted to account for that small difference.

At a prototype pumping rate of 600 cfs and with Froude similarity, the following model parameters were used:

Flow rate through Calumet tunnel	0.818 cfs
Flow rate through one suction header	0.409 cfs
Flow velocity in full flowing Calumet tunnel	0.462 fps
Flow velocity in duct at entrance to wet shaft	0.592 fps
Flow velocity in suction header	2.08 fps
Reynolds number in full Calumet tunnel at water temperature of 40°F	42,000
Reynolds number in suction header at water temperature of 40°F	63,000

Because of the symmetry of the wet shaft and the position of the underground pumphouses, only one wet shaft and one suction header in the west pump room were physically represented in the model. Upstream from the wet shaft the entire system was modeled. A dummy outlet was used to allow for the division of the total flow into two equal amounts. A floor plan of the model layout with major dimension is given in Fig. 5. Drawings of model elements can be provided if desired. Figure 6 is a photograph of the upstream part of the scale model shortly before completion. It shows from right to left the Calumet tunnel, the transition, the drop structure, the divided duct, the wet shaft, and the transition to the suction header. The suction header model, on a temporary support during construction, is shown in Fig. 7. The model of the branch pipe to pump No. 1 is shown in Fig. 8. The valve shown is the one upstream from pump No. 1. The model terminates at the contraction of the branch pipe just upstream from the pump.

Pressure taps connected by tygon tubing to a piezometer board were installed at the following locations:

	Station No.'s
-in the branch pipes at the pump intake downstream from the gate valves	1, 4, 7
-in the branch pipes upstream from the gate valves	2, 5, 8
-on the suction header	3, 6, 9, 10
-on the bottom of the wet shaft sump	11
-on the bottom of the divided duct	13, 14, 15, 16
-in the vertical walls of the box drop structure	17, 18
-in the bottom of the Calumet tunnel	19

The precise locations are shown later in Fig. 46.

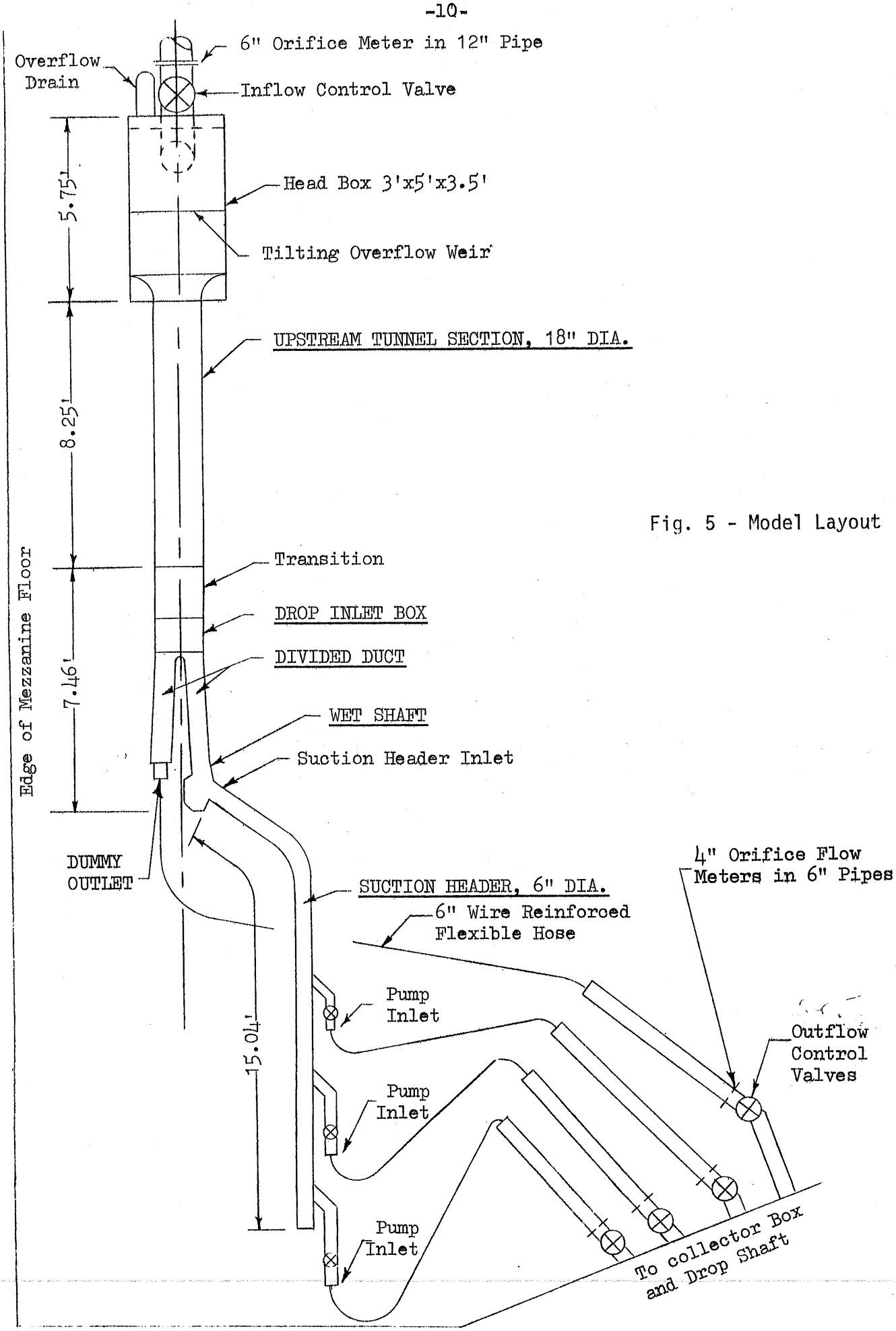

Fig. 5 - Model Layout

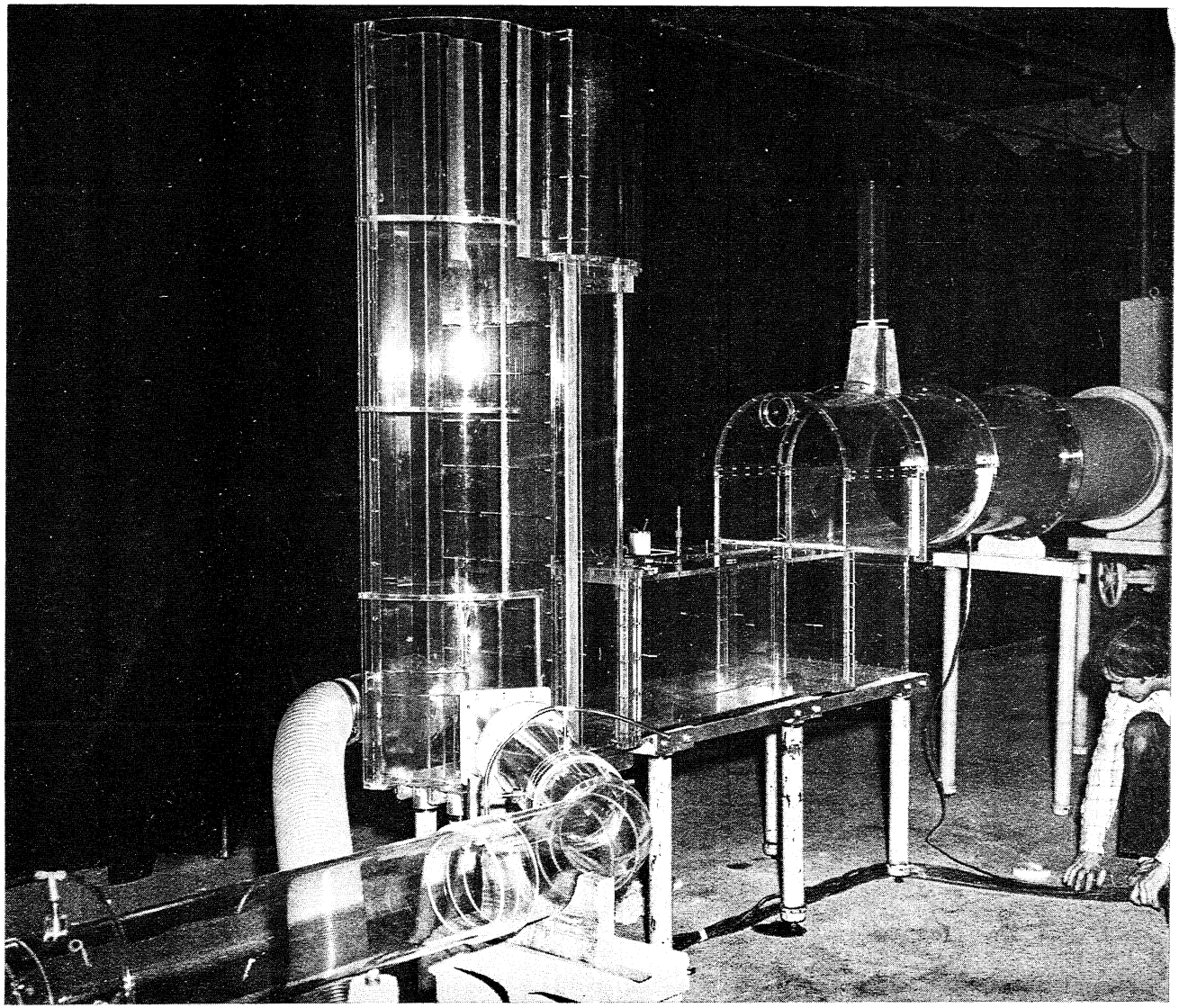

Fig. 6 - Calumet Pumping Station Intake Model. Upstream Part Showing Drop Structure, Divided Duct, Wet Shaft and Suction Header Inlet.

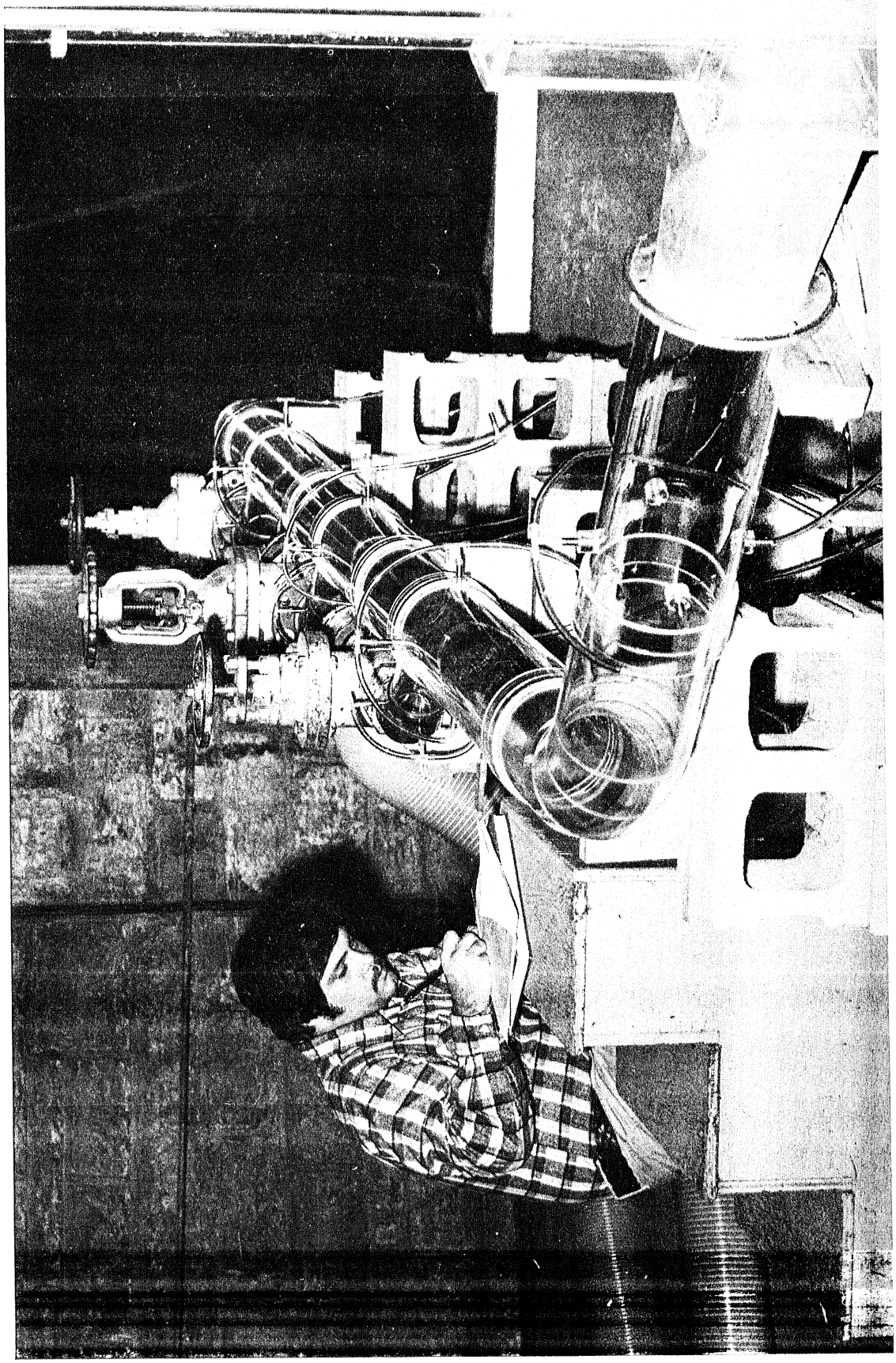

Fig. 7 - Suction Header Model Looking Downstream

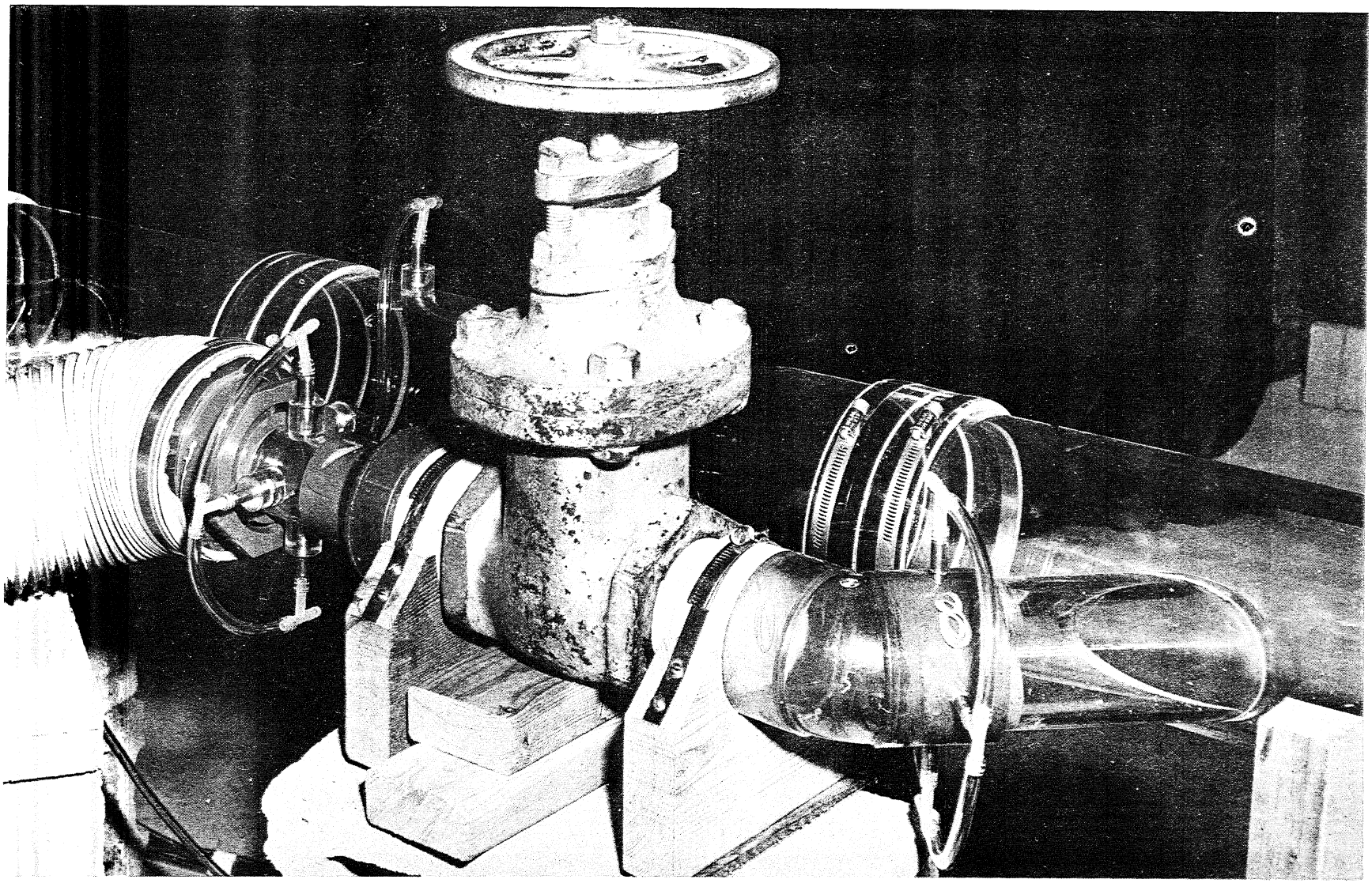

Fig. 8 - Model of Branch Pipe to Pump No. 1. Pressure Taps No. 7 and 8 Upstream and Downstream from Gate Valve.

Flow rates through the branch headers and the suction header were measured by four 4 inch orifice meters installed in 6 inch pipes and controlled by a gate valve downstream from each meter. The total flow into the head box was metered by a 6 inch orifice in the 12 inch main supply pipe. Water surface elevations could be controlled and adjusted by a tilting weir inside the head tank. The gate valves at the end of the branch headers were kept in completely open position and not used for flow adjustments.

As the tests progressed, it became necessary to study, in addition to the original Design A, two design alternatives, Design B and Design C. Modifications were made in the drop structure and the divided duct. In Design B the corner between drop structure and divided duct was rounded ($r = 4.0$ ft) in order to improve the general flow characteristics. In Design C the invert of the divided duct was raised by several feet to reduce its cross-sectional area in order to reduce the potential for grit deposition. The divided duct (influent conduit) in Design C was 7.2 inches shorter in the model than in Designs A and B in order to make it agree with prototype dimensions. The effects of the difference in length were not measurable. The specific geometries of Designs A, B, and C are given in Figs. 9 and 10, respectively.

SCALE MODEL RESULTS

1. Flow Visualization

Confetti or rhodamin WR were used alternatively for flow visualization. Entrained air bubbles, where present, also showed flow patterns. Experiments with the original design discharge of 600 cfs and wet shaft W.S. elevation of -320 or above showed the following:

a. Flow through the suction header had a small secondary swirl induced by the 135° bend. Flow into the branch headers of the pumps seemed satisfactory. No major separation regions were apparent.

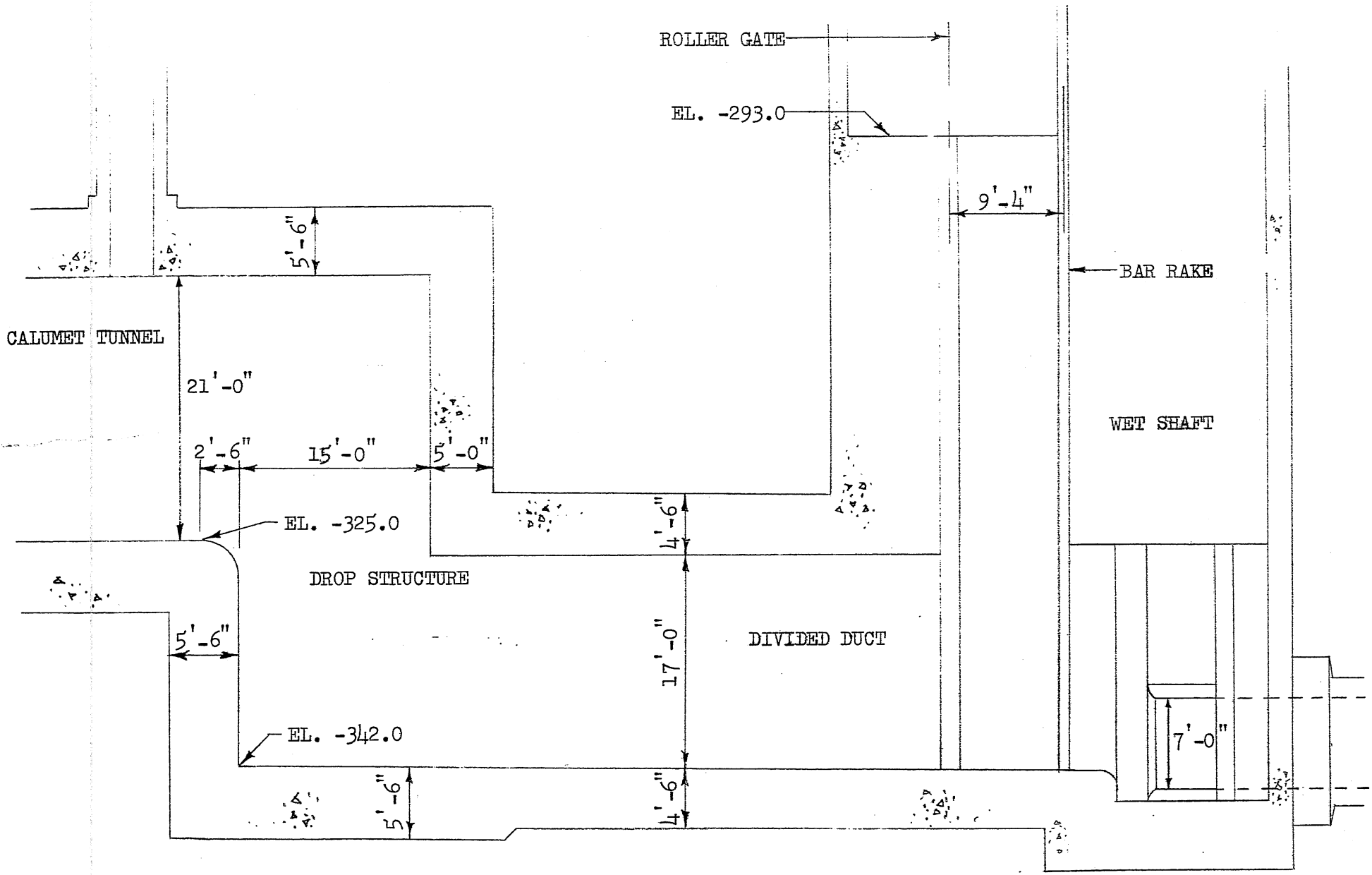

Fig. 9 - Design A (original) of Drop Structure, Divided Duct and Wet Shaft.

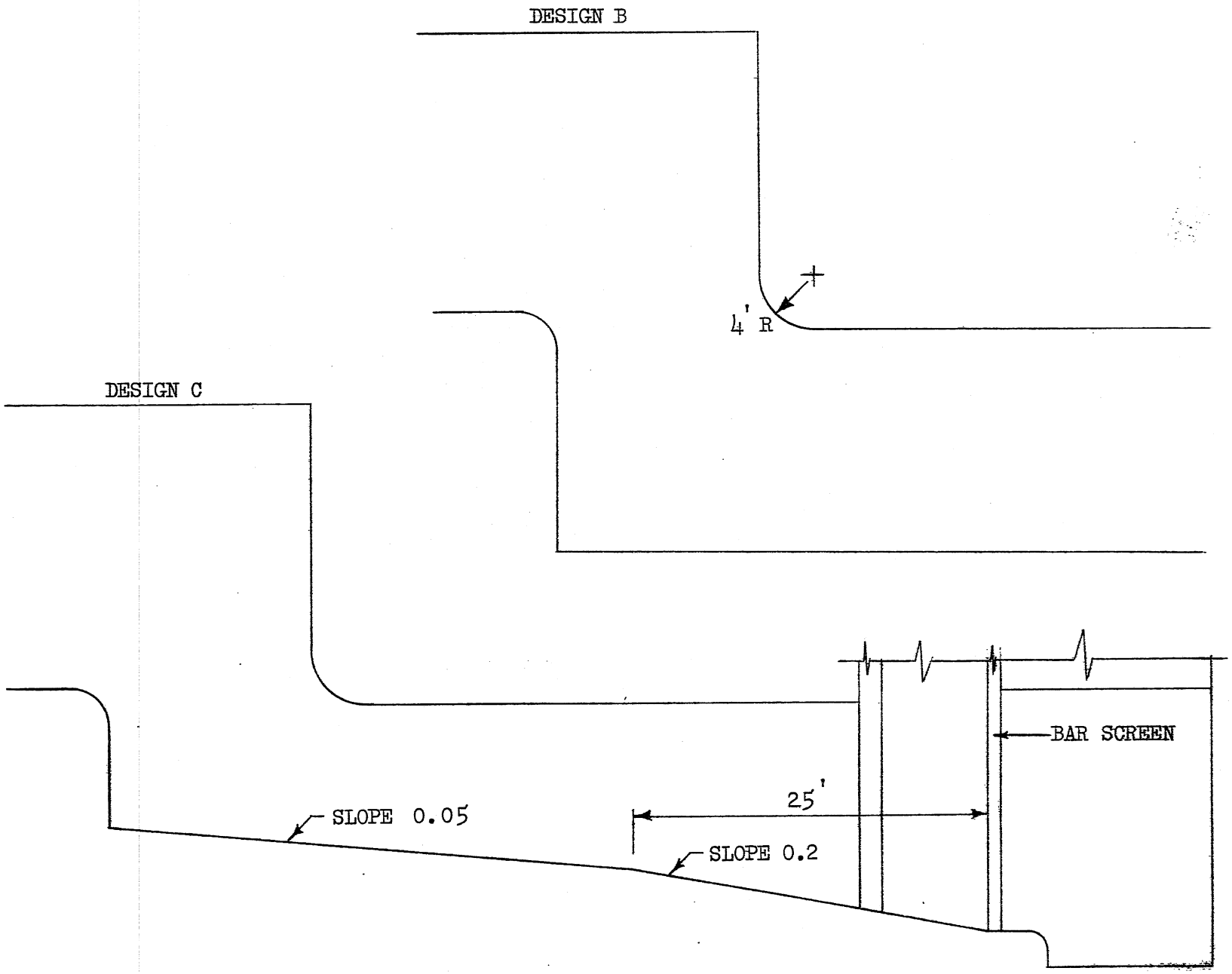

Fig. 10 - Design B and Design C of Drop Structure and Divided Duct.

b. Flow from the wet shaft into the suction header seemed satisfactory, with only a minor separation region above the suction header intake (upper left corner looking in flow direction).

c. Flow from the divided duct into the wet shaft and through the bar screen was somewhat faster near the bottom but in a forward direction over the total height. The water surface in the wet shaft was quite calm without indication of any major vortex formation. Figure 11 shows the situation.

To simulate a clogged trash rake, paper chips 2.3' x 2.3' in size were added to the water. These particles were found to deposit randomly on the trash rake. As more particles were deposited, the water surface elevation downstream from the rake dropped. With approximately 85 percent of the rake area covered, the flow configuration shown in Fig. 12 was observed. Approximately 66 pieces representing a combined surface area of 350 ft^2 had deposited, with overlap, on 207 ft^2 of trash rake area to produce the situation. Flow velocities through the remaining openings were increased to several times their value for unobstructed conditions. The turbulence in the wet shaft downstream from the rake was thereby increased drastically. However, no vortex formation or air entrainment into the suction header was produced.

d. Flow through the box drop structure was very adversely affected by the 90° corner between the end wall of the structure and the crown of the divided duct. At that corner flow was essentially directed downward instead of horizontally into the duct. When the water stages in the Calumet tunnel were high enough and the approach velocities small, the region of separated flow downstream

Fig. 11 - Flow from Divided Duct through Unobstructed Bar Screen into Suction Header.

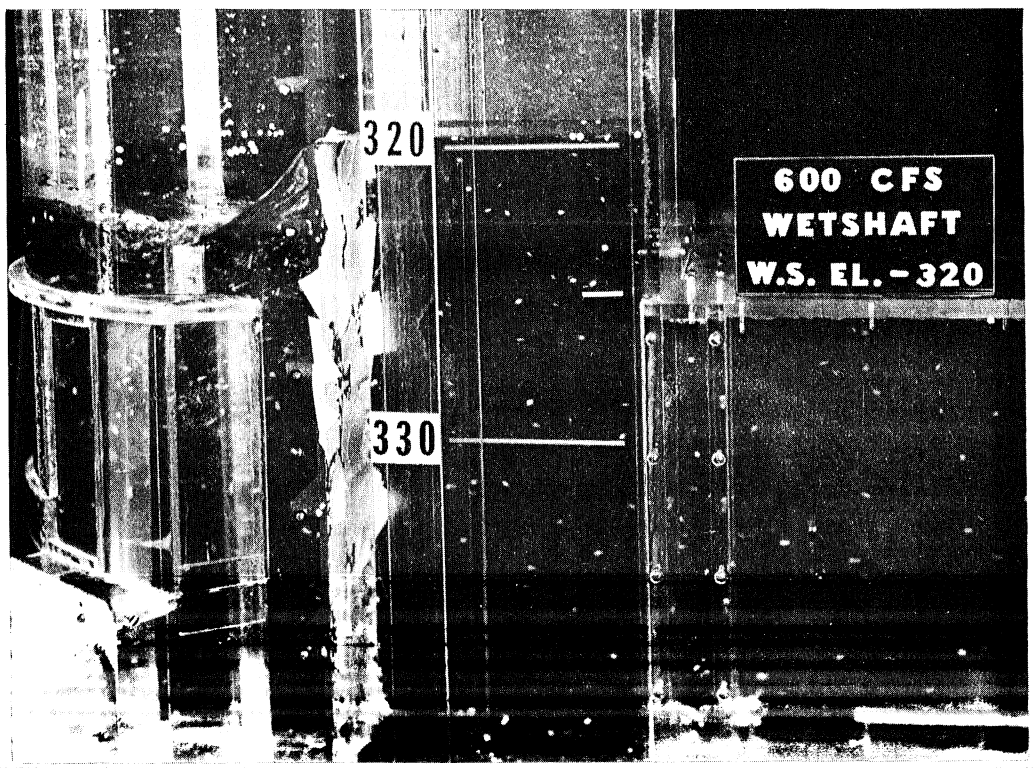

Fig. 12 - Flow through Uniformly Obstructed Bar Screen.

from the corner was not particularly prevalent, as shown in Fig. 13. At very low stages, the situation worsened considerably. A downward jet flow developed and the separation region carried far into the duct as seen in Fig. 14.

As a result of these observations, it was decided to replace the sharp 90° corner with a rounded one (Design B). A prototype radius of 4 ft was used. Flow patterns through the modified structure are shown in Figs. 15 through 21. Flow conditions were largely improved.

Subsequently, the height of the duct was reduced for reasons related to grit transport (Design C). This made mean flow velocities in the duct more uniform but did not change the flow pattern appreciably compared to those given in Figs. 15 to 21.

The flow pattern for the final design is shown in Fig. 22, for the full flowing tunnel. Suspended confetti again illustrates the streamlines. A separation zone is still present in the drop structure at the end of the tunnel, but the overall flow into the duct is quite satisfactory. Flow conditions at lower stages and full pumping rate are shown in Figs. 23 and 24. By comparison with full flowing conditions, much higher turbulence levels are observed. The separation zone has become less distinct. Some secondary vortex type motion near the water surface is also apparent in Fig. 24.

2. Air Entrainment

When slugs of air are drawn into a pump, very serious operational problems and failures can develop. Air entrainment under several different operating conditions and in different parts of the model therefore had to be examined, including

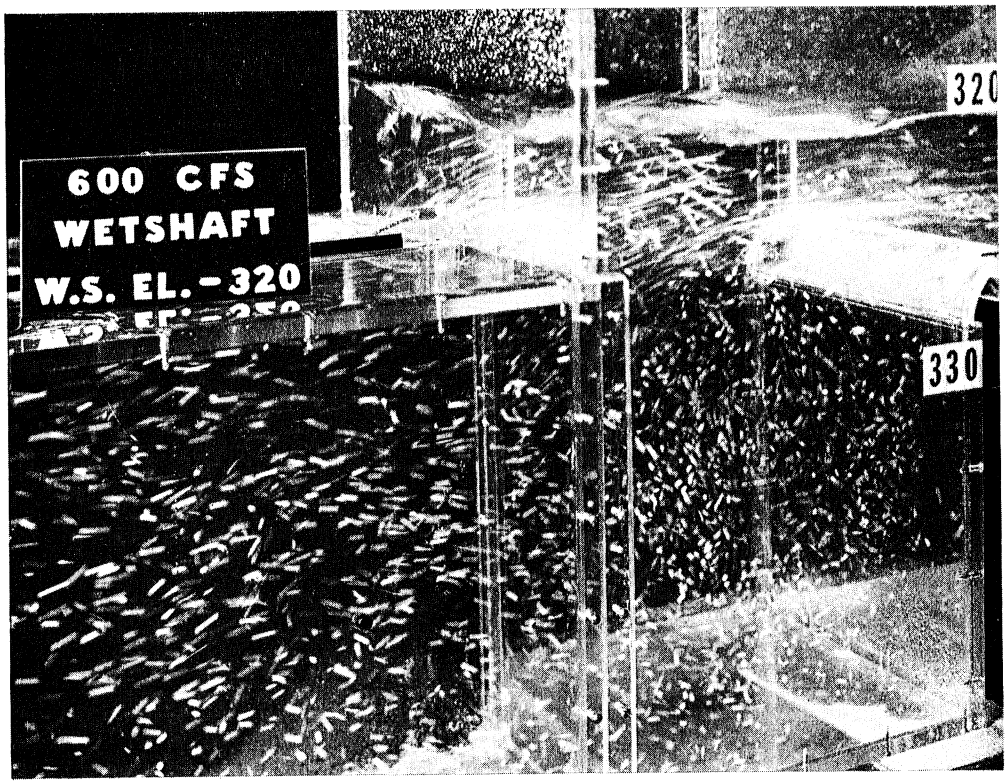

Fig. 13 - Flow Visualization in Drop Structure at Low Stage Using Suspended Confetti Particles. Design A.

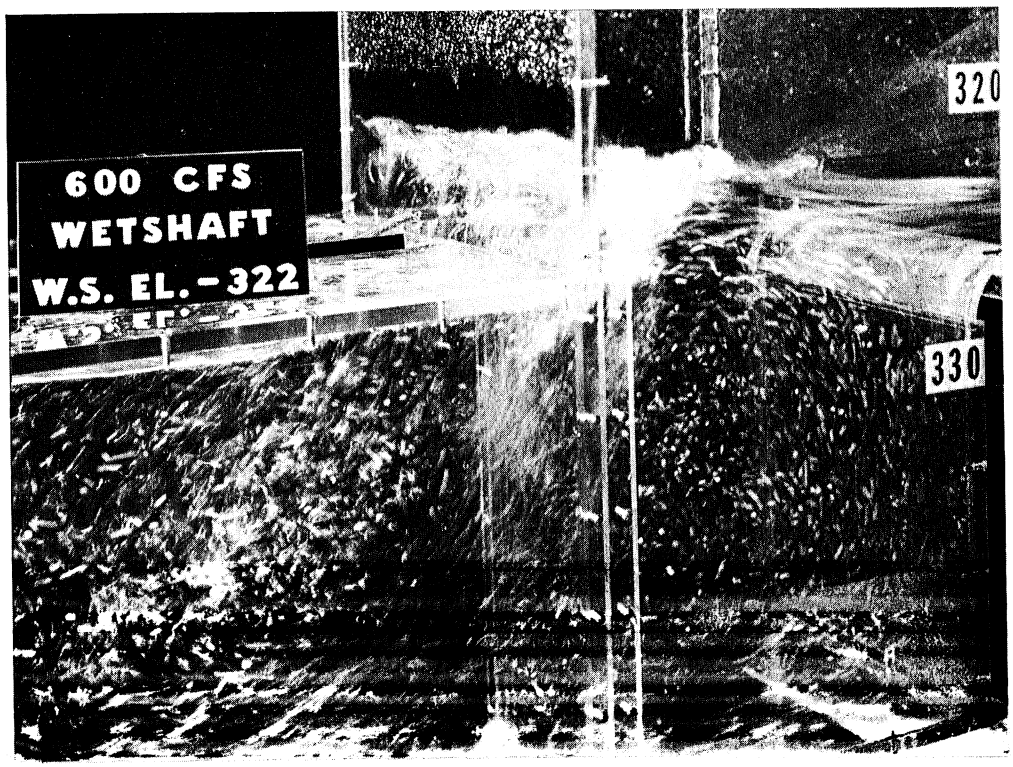

Fig. 14 - Flow Visualization in Drop Structure at Low Stage Using Suspended Confetti Particles. Design A.

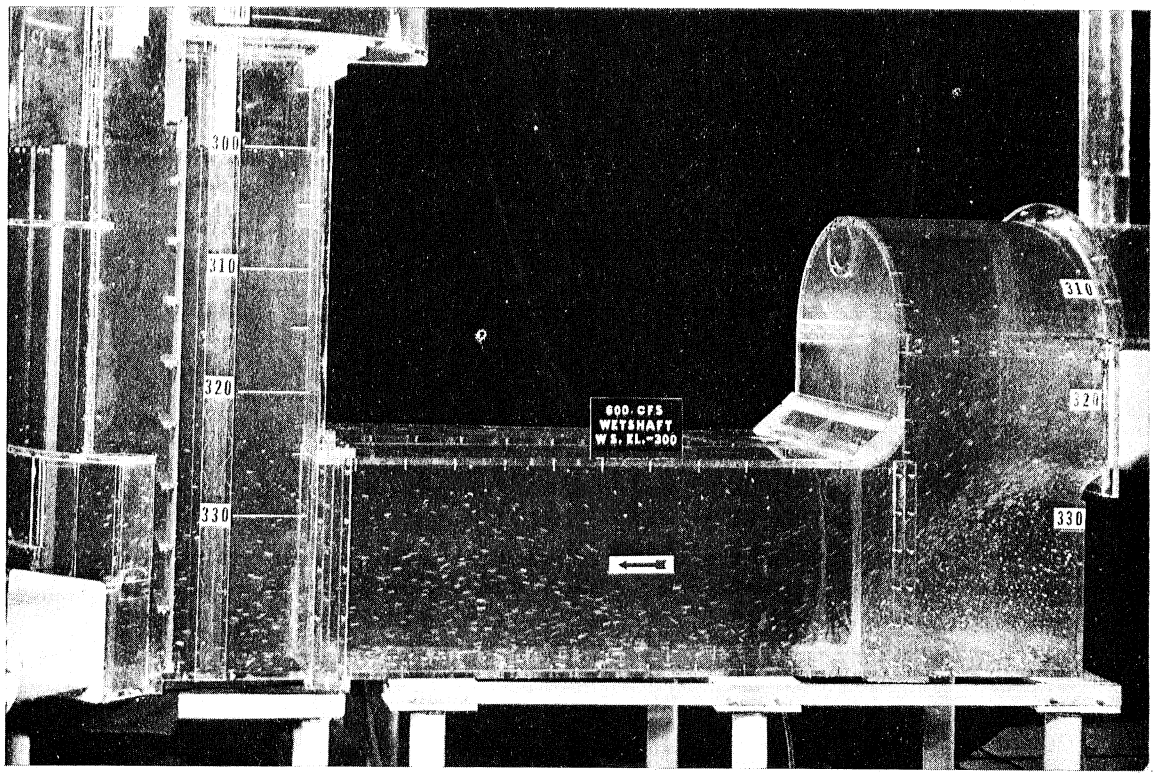

Fig. 15 - Flow Visualization in Drop Structure, Divided Duct and Wet Shaft at High Stage Using Suspended Confetti Particles.

Fig. 16 - Detail of Flow Visualization at High Stage Showing Large Separation Region in Drop Structure and High Velocities near Crown of Divided Duct.

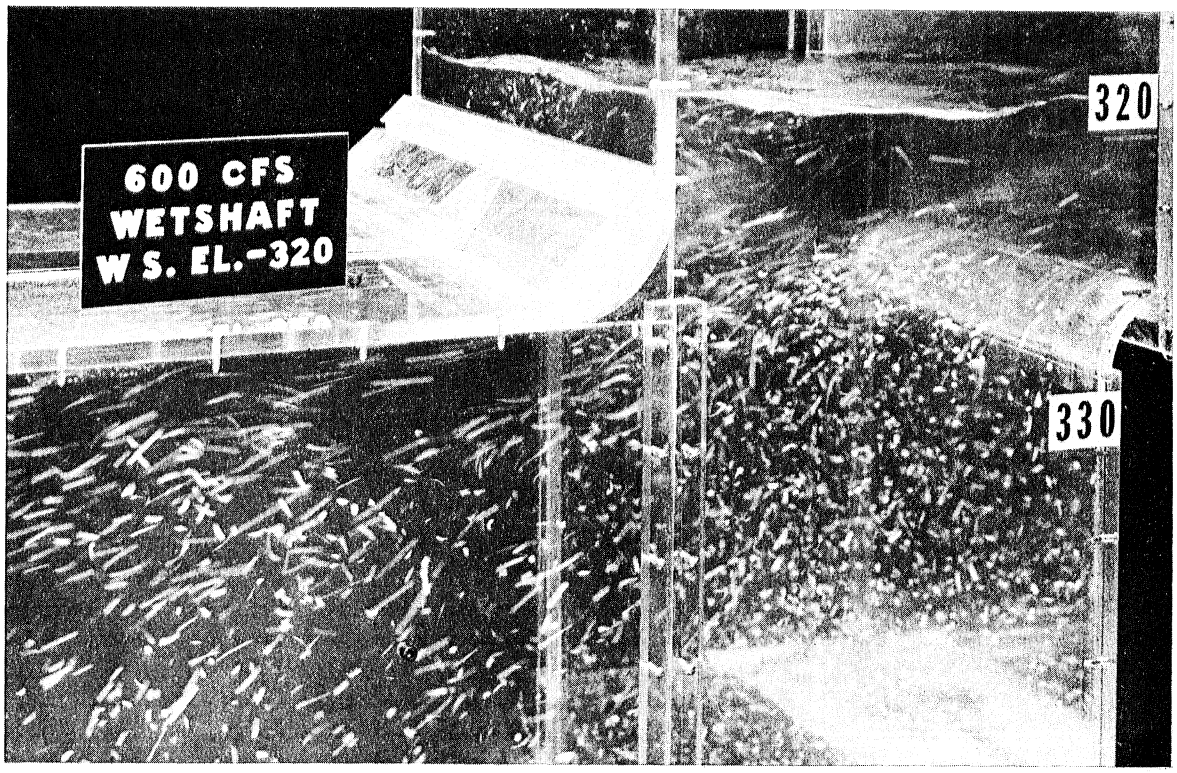

Fig. 17 - Flow Visualization of Transition from Drop Structure to Divided Duct at Low Stage. Design B.

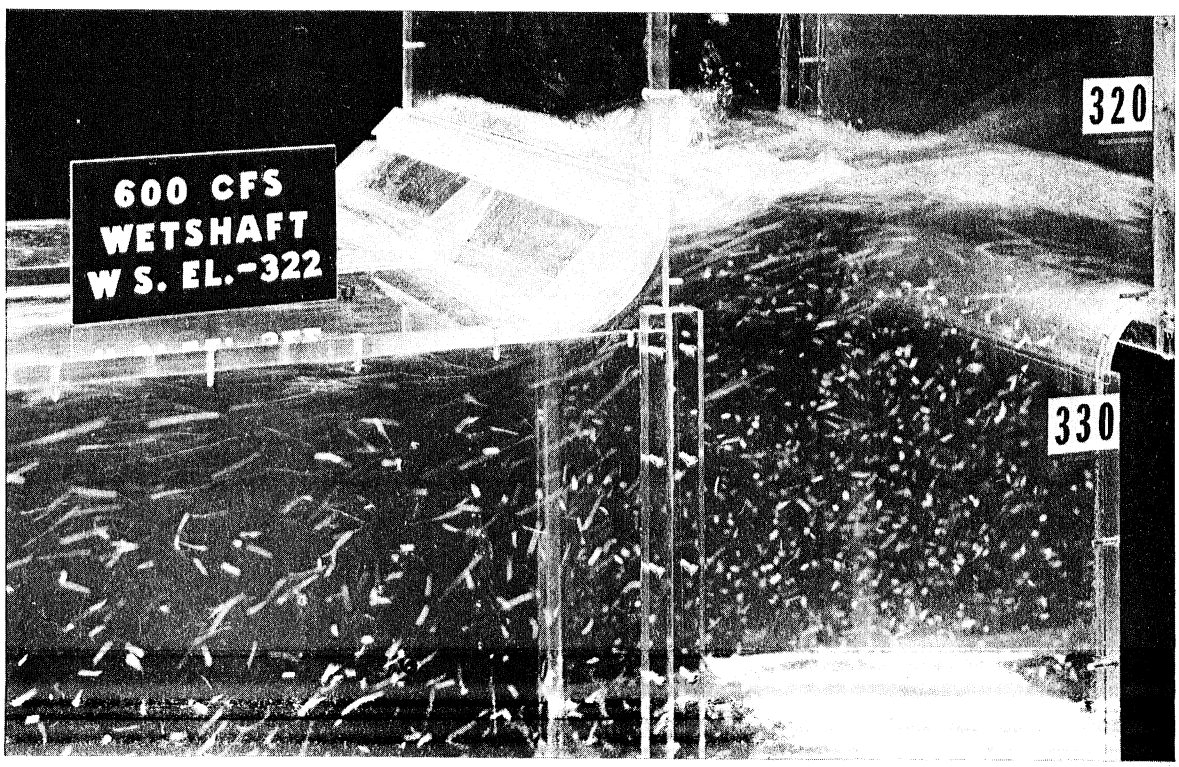

Fig. 18 - Flow Visualization of Transition from Drop Structure to Divided Duct at Low Stage. Design B.

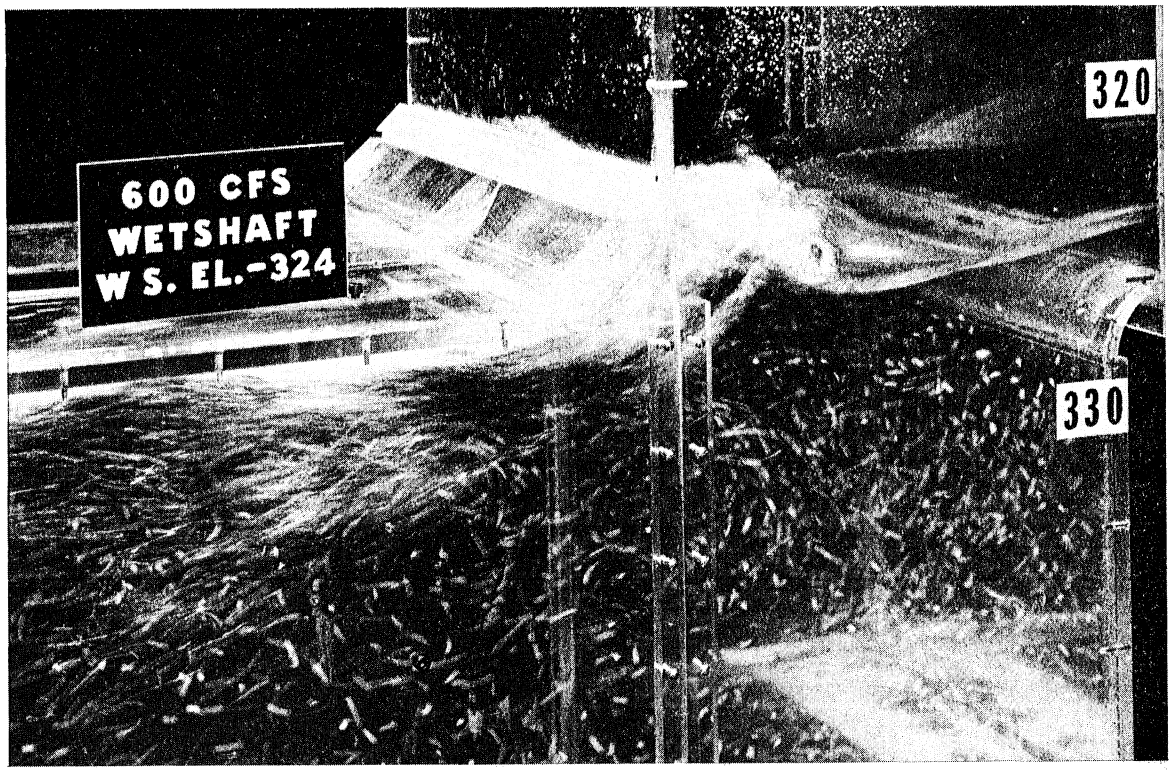

Fig. 19 - Flow Visualization of Transition from Drop Structure to Divided Duct at Low Stage. Design B.

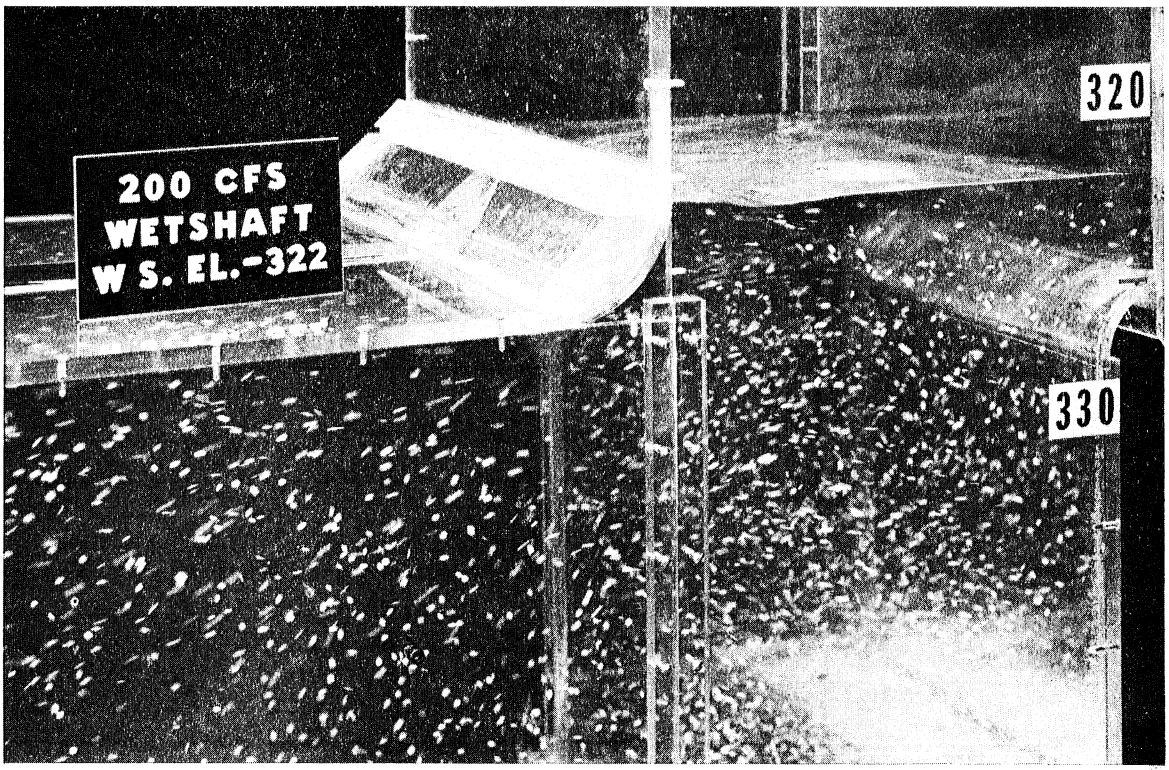

Fig. 20 - Flow Visualization of Transition from Drop Structure to Divided Duct at Low Stage. Design B.

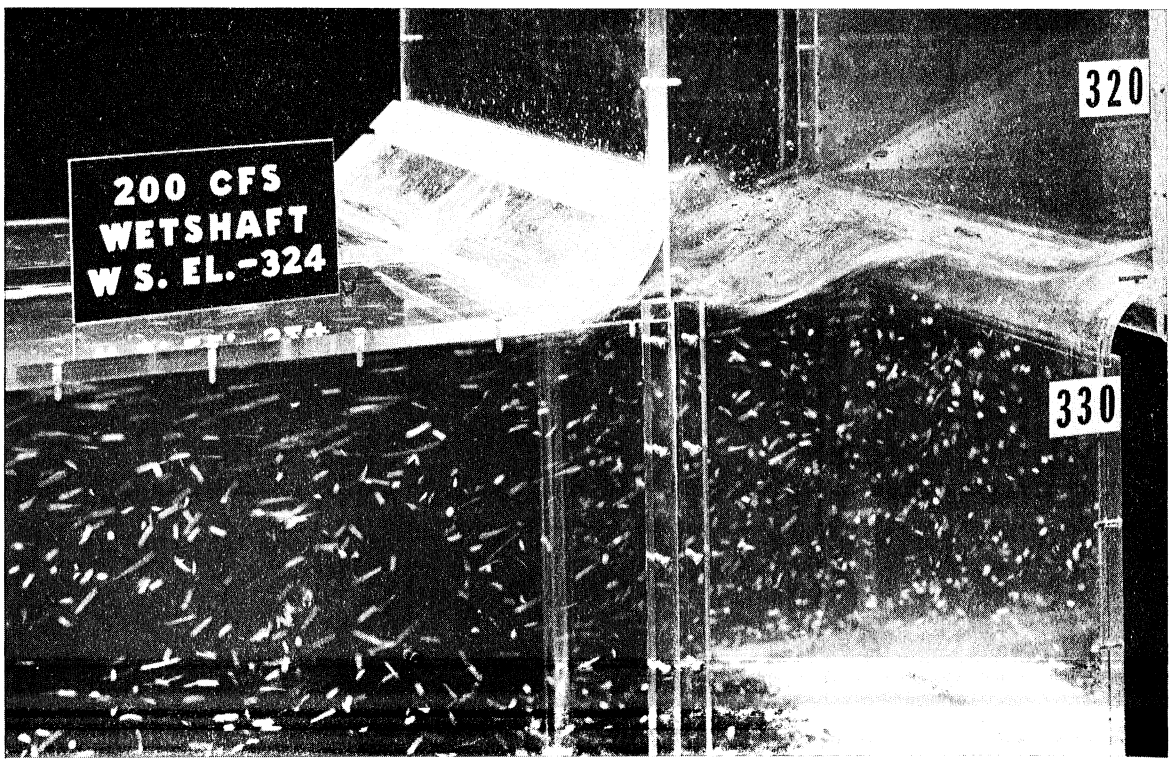

Fig. 21 - Flow Visualization of Transition from Drop Structure to Divided Duct at Low Stage. Design B.

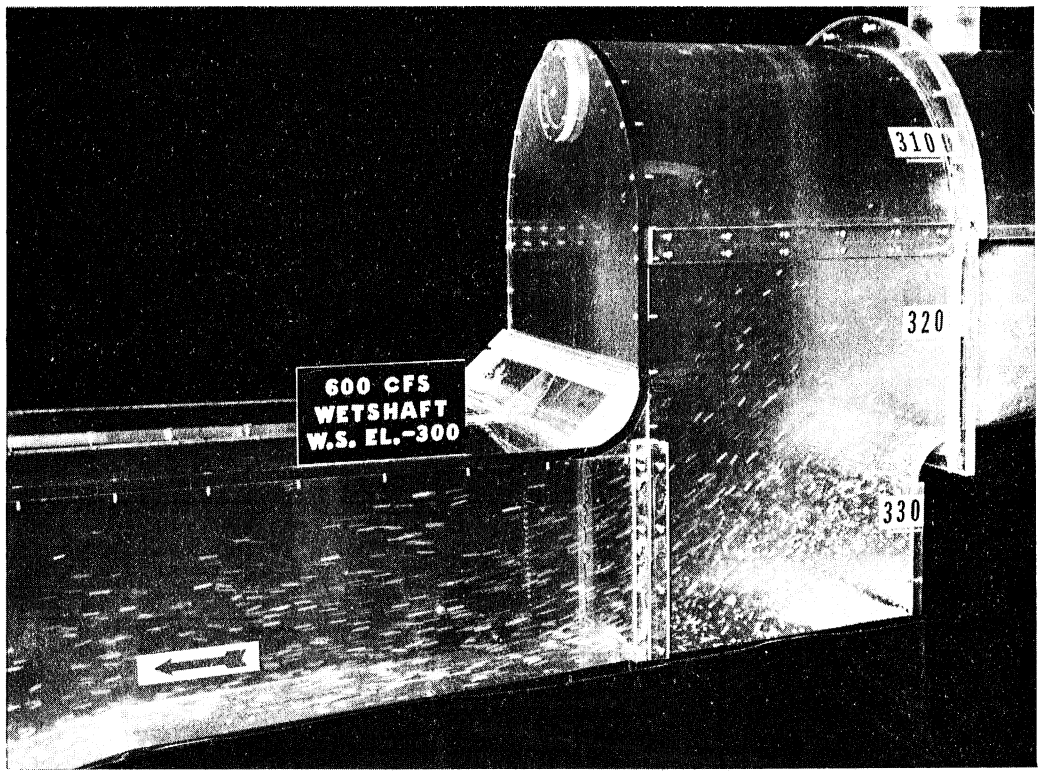

Fig. 22 - Flow Visualization in Drop Structure and Divided Duct at High Stage Using Suspended Confetti Particles. Design C.

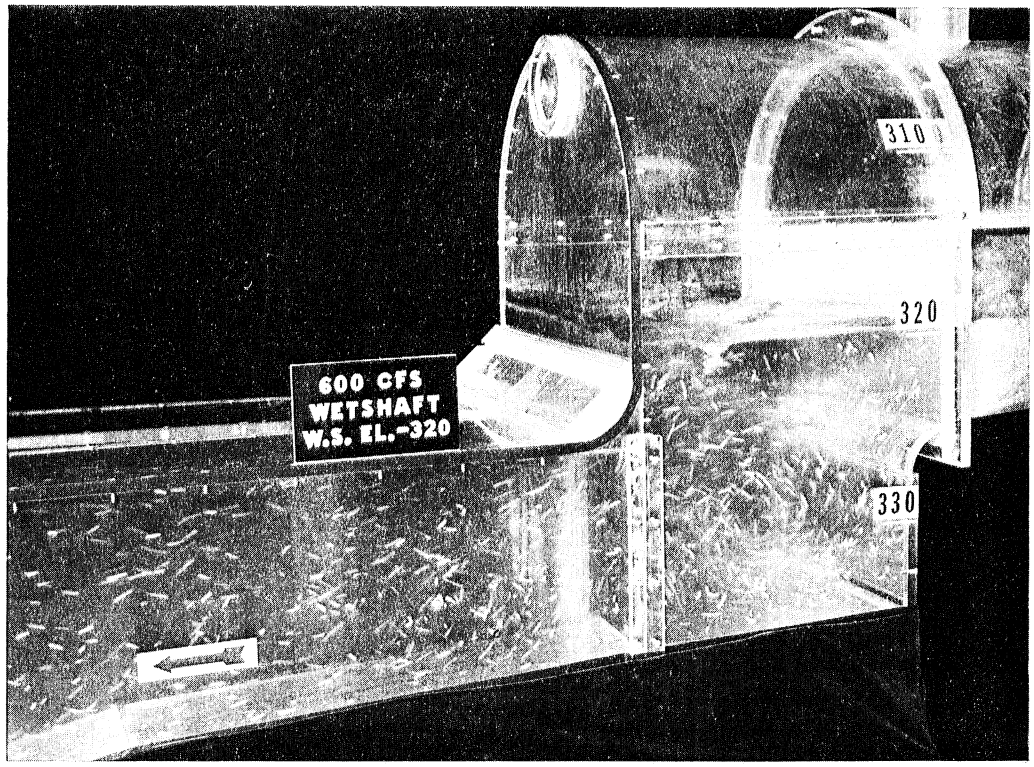

Fig. 23 - Flow Visualization in Drop Structure and Divided Duct at Low Stage Using Suspended Confetti Particles. Design C.

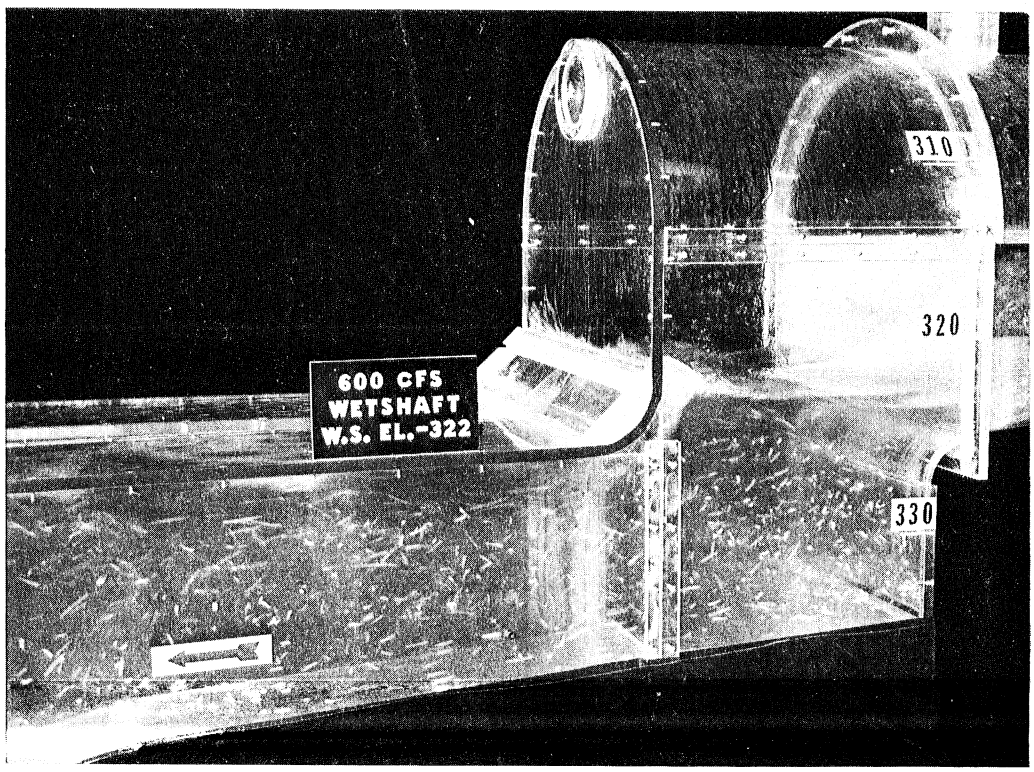

Fig. 24 - Flow Visualization in Drop Structure and Divided Duct at Low Stage Using Suspended Confetti Particles. Design C.

- Entrapment of air pockets during filling of suction headers and subsequent entrainment during pump start-ups.
- Vortex formation and air entrainment in wet shaft under normal operation near 600 cfs and stages near or below -320.
- Drawdown of wet shaft below normal operating water stages and air entrainment when wet shaft is being emptied.
- Vortex formation and other secondary flows and turbulence resulting in air entrainment from box drop structure at low stages.

2.1 Filling of Suction Header and Air Entrainment During Pump Start-up.

The first experiments were conducted without air vents installed on the suction header. It was observed that air was trapped along the crown of the suction header when it was filled very slowly. The air pocket extended on the order of 0.15 inches below the crown and over almost the total length of the suction header. If scaled purely geometrically, the initial air bubble in the prototype would extend over a height of 0.18 ft, occupy an area of about 0.59 ft^2, and have a volume of approximately 124 ft^3. However, surface tension is responsible for keeping the initial air pocket in the pipe and Weber numbers are not the same in the prototype and in the model. The dimensions and the volume of the prototype bubble will therefore be smaller than indicated by purely geometrical scaling. It is estimated that the prototype bubble height h will scale with a factor of no more than 6.0. The prototype bubble height at its formation will be no more than 0.9 inches and the trapped air volume will be no more than 15 ft^3. At increasing water stages the bubble will be further compressed, more so in the prototype than in the model.

When pump No. 1 (50 cfs) is turned on, the air bubble along the crown of the suction header is somewhat compressed, as shown in Fig. 25. No air is drawn into the pump. When pump No. 2 is started, bringing the total flow

through the suction header to 175 cfs, the air bubble along the crown is further shortened, as shown in Fig. 26, but no air is drawn into pump No. 2. Finally, and immediately after pump No. 3 has been started, the entrapped air bubble is moved downstream and air is drawn into pumps No. 1 and 2 but not into pump No. 3. The final bubble configuration when no more entrainment occurs under full flow of 300 cfs in the suction header is shown in Fig. 27.

To prevent any air entrainment into the pumps during the start-up process, it is recommended to install air vents on top of the suction header at three locations. The most suitable locations have been found to be the intersections of the branch pipe axis and the main suction header wall. The vents should be of sufficient size to allow evacuation of the entrapped air volume within the period of the pump start-up.

2.2. Air Entrainment by Vortex Formation in Wet Shaft

Under normal operating conditions and for total flows up to 600 cfs and wet shaft water surface elevations down to -324.0, no significant vortex formation in the wet shaft and no air entrainment were observed. Using the vortex classification given in Fig. 28, the following flow conditions were noted:

Total Pumping Rate (cfs)	Wet Shaft Water Surface Elevation	Vortex Classification Number
600	-320 and above	1
600	-322	2
600	-324	2
400	-322 and above	1
400	-324	2
200	-324 and above	1

Random obstruction of the trash rake, up to 85 percent, did not cause vortex formation in the wet shaft or air entrainment into the suction header.

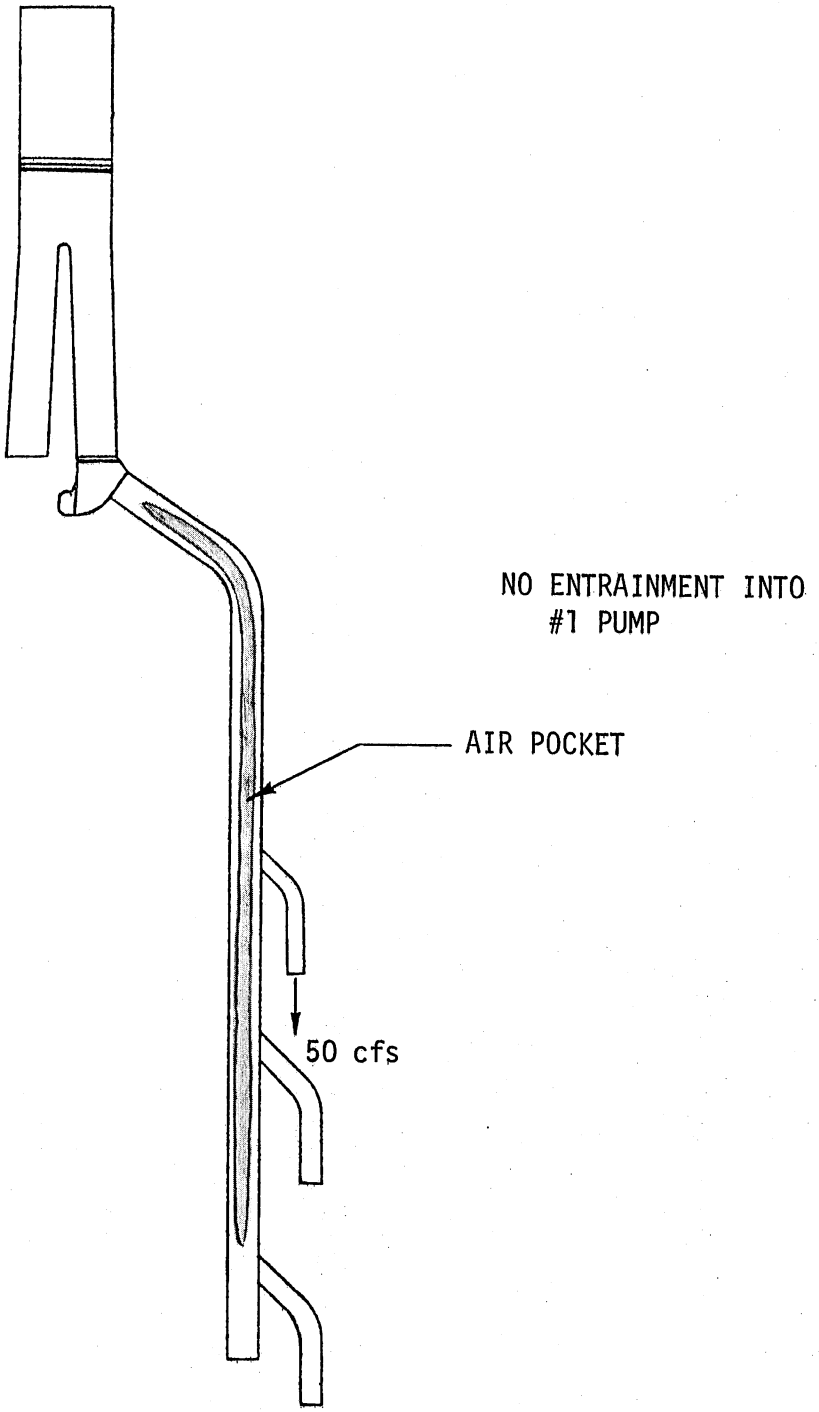

Fig. 25 - Extent of Air Pocket in Suction Header (Plan View) During Filling. Pump No. 1 Operating at 50 cfs.

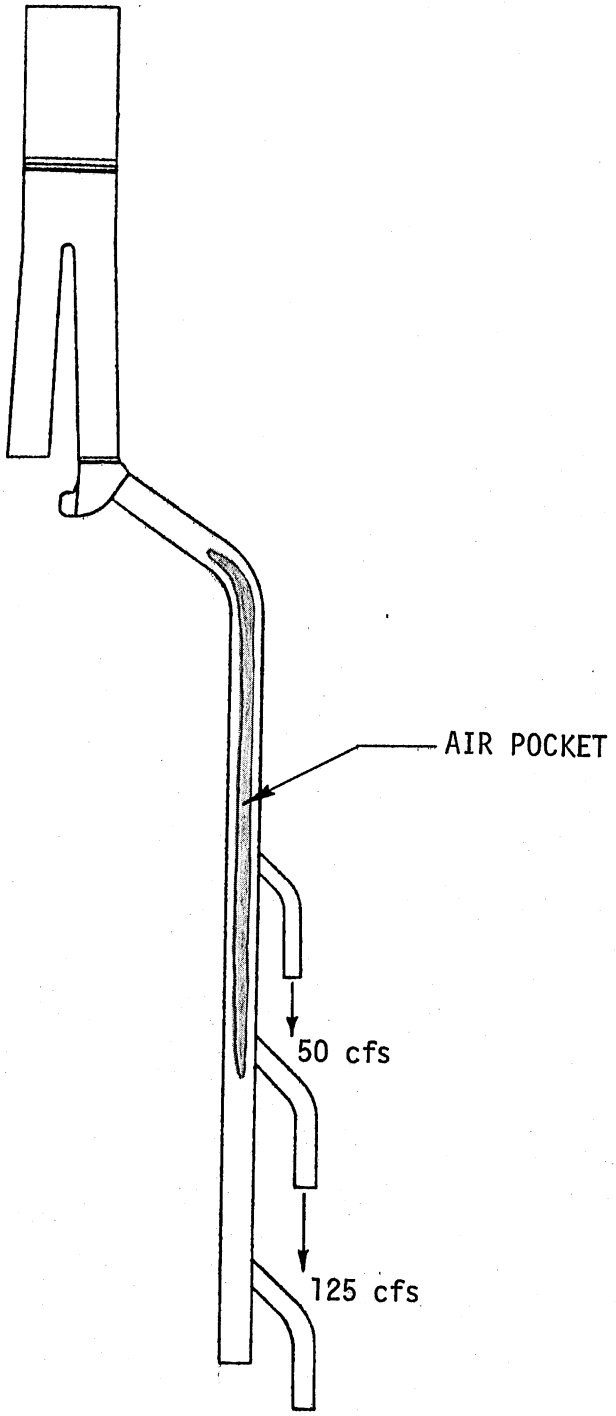

Fig. 26 - Extent of Residual Air Pocket in Suction Header (Plan View) After Pump No. 1 and No. 2 have been started.

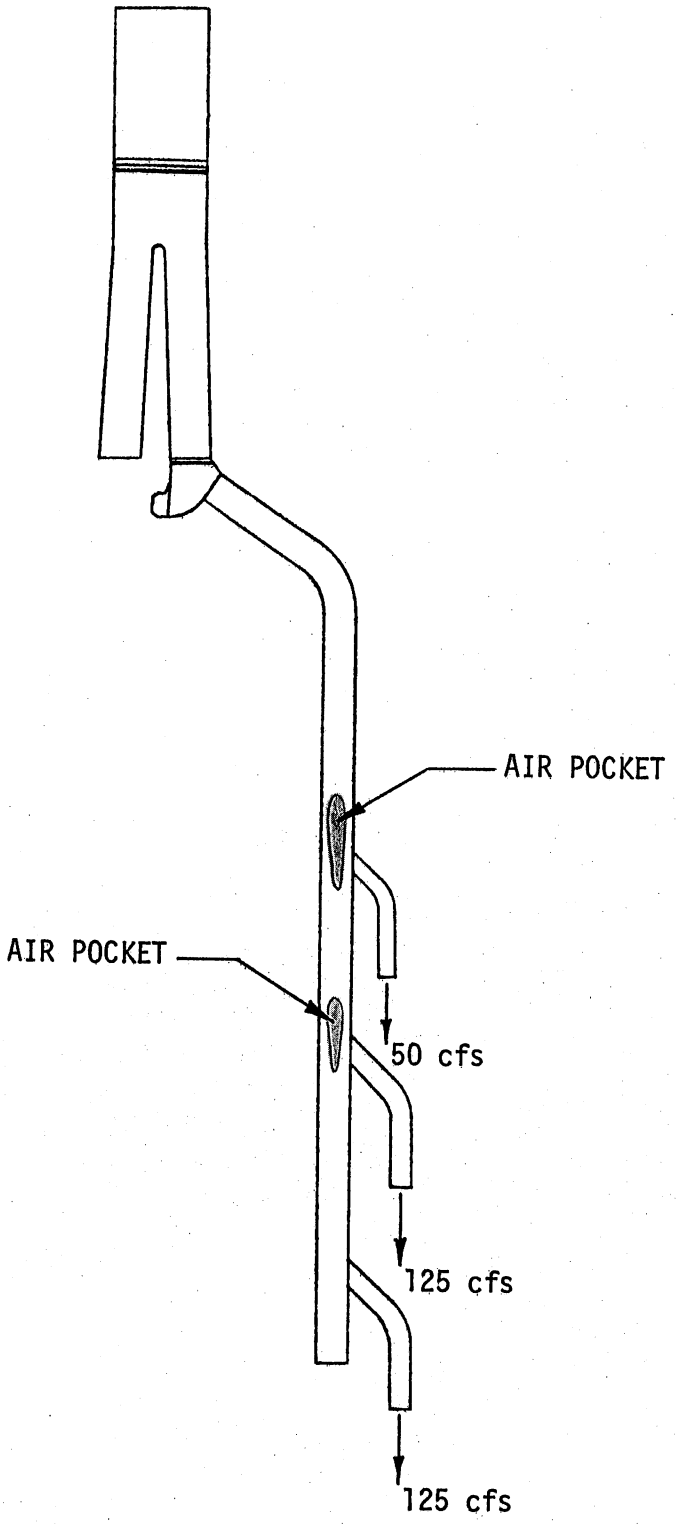

Fig. 27 - Extent of Residual Air Pockets in Suction Header (Plan View) After Pumps No. 1, 2, and 3 have been started.

#1 Surface Rotation Without Depression

#2 Surface Rotation With Slight Surface Depression

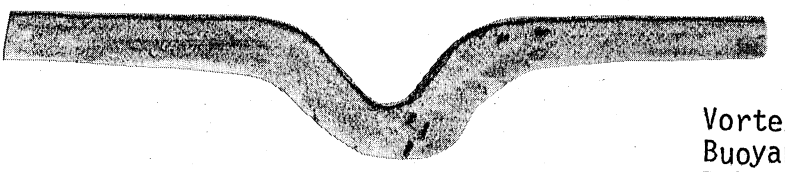

#3 Vortex Pulls Down Buoyant Surface Debris

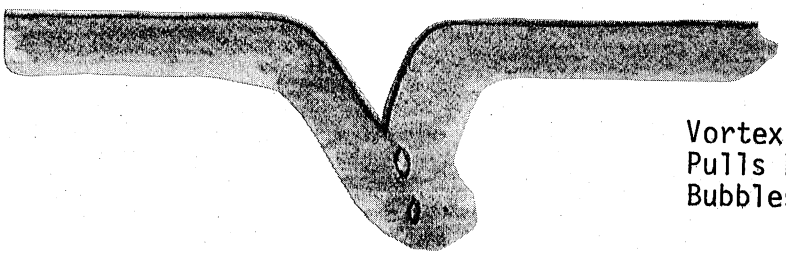

#4 Vortex Intermittently Pulls Down Air Bubbles

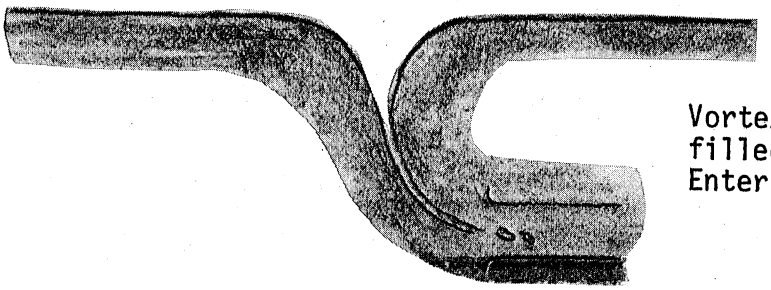

#5 Vortex Core Air-filled With Air Entering Pipe

Fig. 28 - Vortex Classification System

Heavy sediment (grit) deposition in the divided duct, as shown and discussed in a later section, did not cause any vortex formation or air entrainment from the wet shaft.

The one and only observation of a severe vortex in the wet shaft (class #3 to 5 in Fig. 28) was made when a complete obstruction of the lower portion of the trash rake was simulated by covering the lowermost 10 x 9 ft of the trash rake with a board in the model. The resulting strong upward velocity component caused high flow velocities near the water surface (elevation -322) which in turn produced the vortex formation. To prevent this situation in the prototype, the lowermost portion of the trash rake must be kept as clean as the rest of the rake.

2.3. Air Entrainment During Drawdown of Wet Shaft Water Level with Pump No. 1

Drawdown of the water in the wet shaft, e.g. for maintenance or other works can be accomplished in several different ways. An experiment using pump No. 1, with a pumping rate of 50 cfs, was conducted. During the drawdown the water surface in the wet shaft remained perfectly smooth. When the stage dropped to the crown of the suction header, a wave travelled rapidly down the header. At the same time a wave formed at each air vent, travelling upstream. No air entrainment into pump No. 1 occurred until the water surface elevation in the main suction header reached the crown of the branch header, while a pumping rate of 50 cfs was maintained.

2.4. Air Entrainment from Box Drop Structure During Low Stages

At low stages the flow out of the box drop structure and into the divided duct, such as shown in Figs. 14, 18, 19, 21, and 24 is associated with significant air entrainment. The formation of a roller or of standing waves and a certain amount of vorticity due to the non-uniform velocity distribution of the flow out of the tunnel make the air entrainment possible.

The situation at two flow rates and stages for the original Design A. is shown in Figs. 29 through 32.

After the downstream corner had been rounded (Design B), the situation was somewhat changed. Air entrainment still occurred at about the same water stages, but the air bubbles were carried closer to the crown of the divided duct structure. The transition from a non-air entraining condition to an entraining one is shown in Figs. 33 through 37 for flows of 600 cfs and 400 cfs. As to be expected, the amount of air entrained diminishes as the pumping rates are lowered. At 50 cfs flow, no more air entrainment occurred into the divided duct structure.

In the original design and at higher flows, air was entrained in bubbles which coalesced near the crown of the structure and were released in the form of major 'burps' into the wet shaft. The rounding of the corner resulted in less air accumulation under the crown. Some very finely dispersed small bubbles were also formed. They appeared, if at all visible, to be uniformly dispersed in the water and of no consequence for pump operation. Air entrainment conditions for Design C are shown in Figs. 38 through 45.

The following operating stages for air entrainment from the drop structure into the divided duct were observed in the model for Design B and Design C.

Wet Shaft Water Surface Elevation (ft)

Total Pumping Rate (cfs)	No Air Entrainment	Some Air Entrainment	Full Air Entrainment
600	-320	-321	-322
400	-321	-322	-323
200	-322	-323	-324
50	-324		

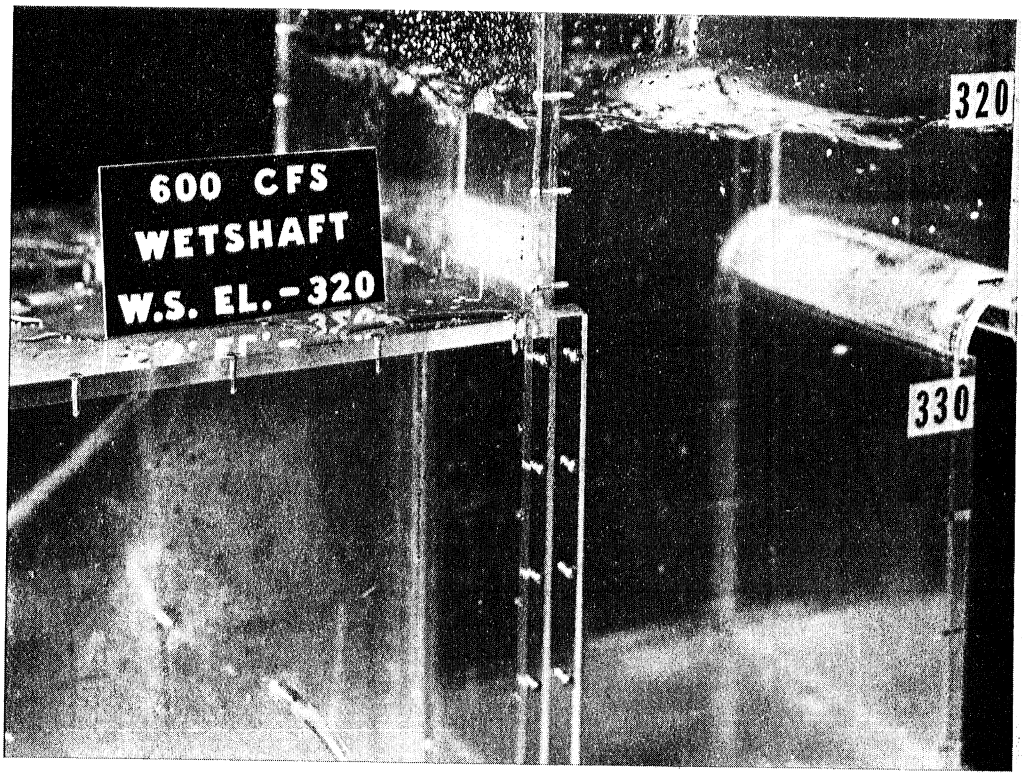

Fig. 29 - Free Surface Configuration in Drop Structure at Low Stage. Design A.

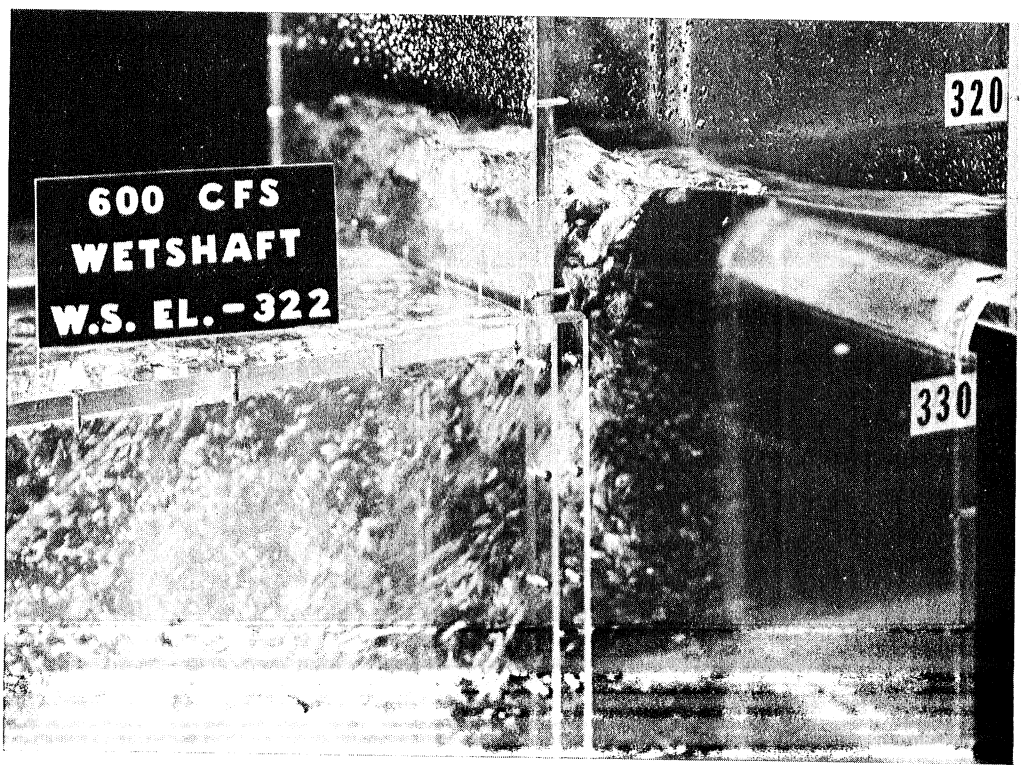

Fig. 30 - Air Entrainment and Free Surface Configuration in Drop Structure at Low Stage. Design A.

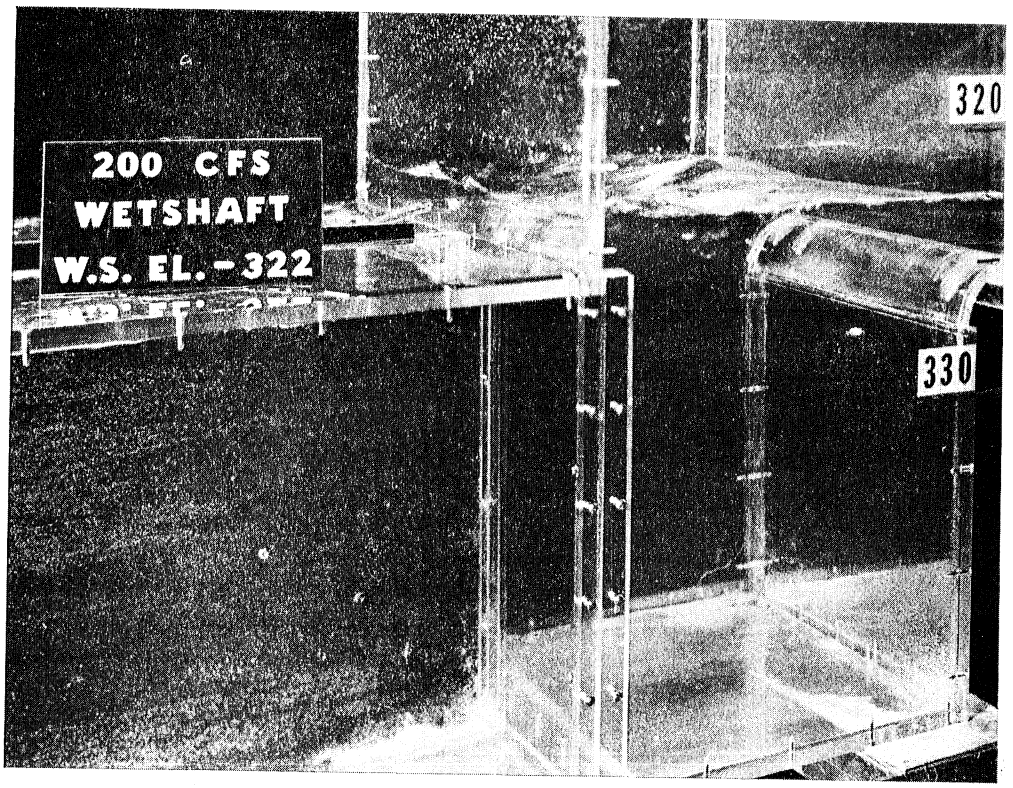

Fig. 31 - Free Surface Configuration in Drop Structure at Low Stage. Design A.

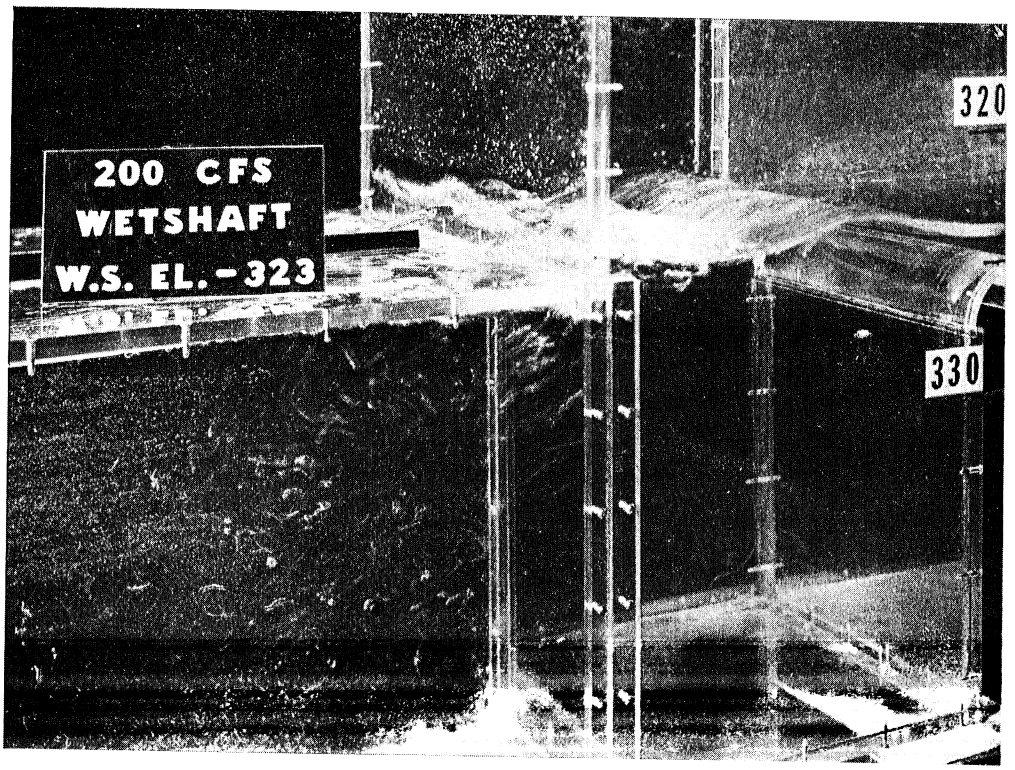

Fig. 32 - Air Entrainment and Free Surface Configuration in Drop Structure at Low Stage. Design A.

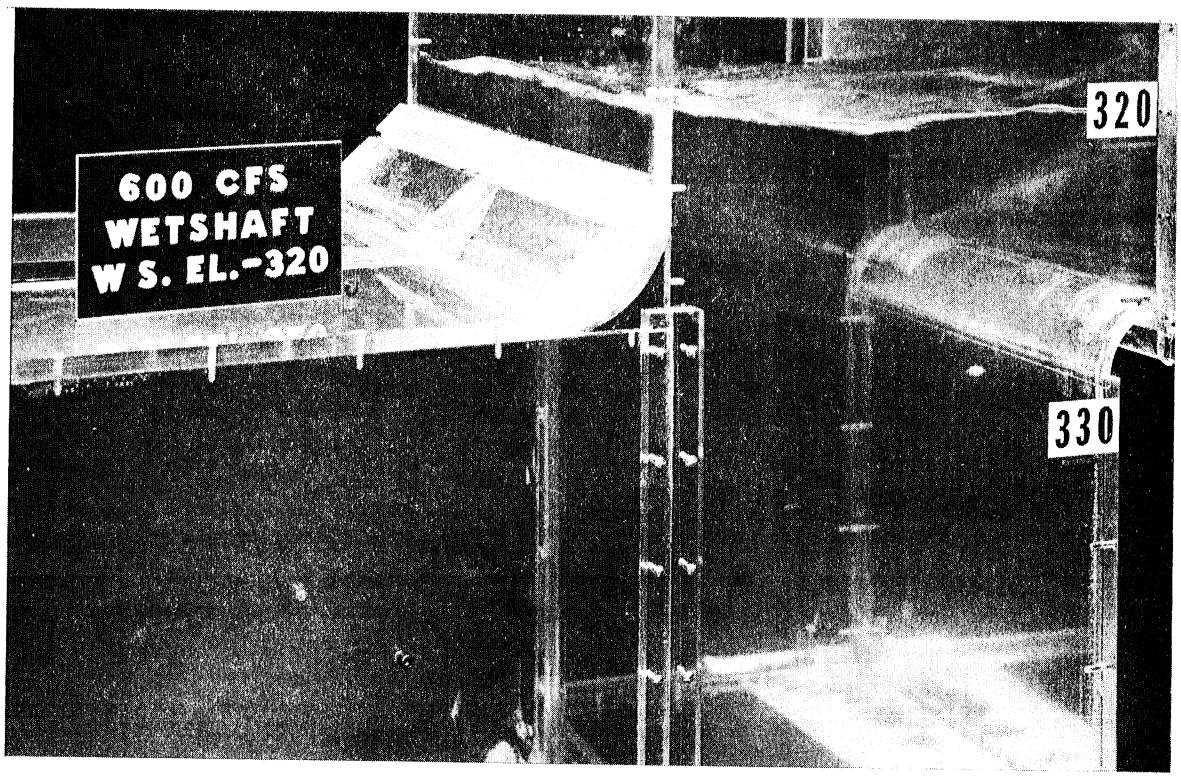

Fig. 33 - Free Surface Configuration in Drop Structure at Low Stage. Design B.

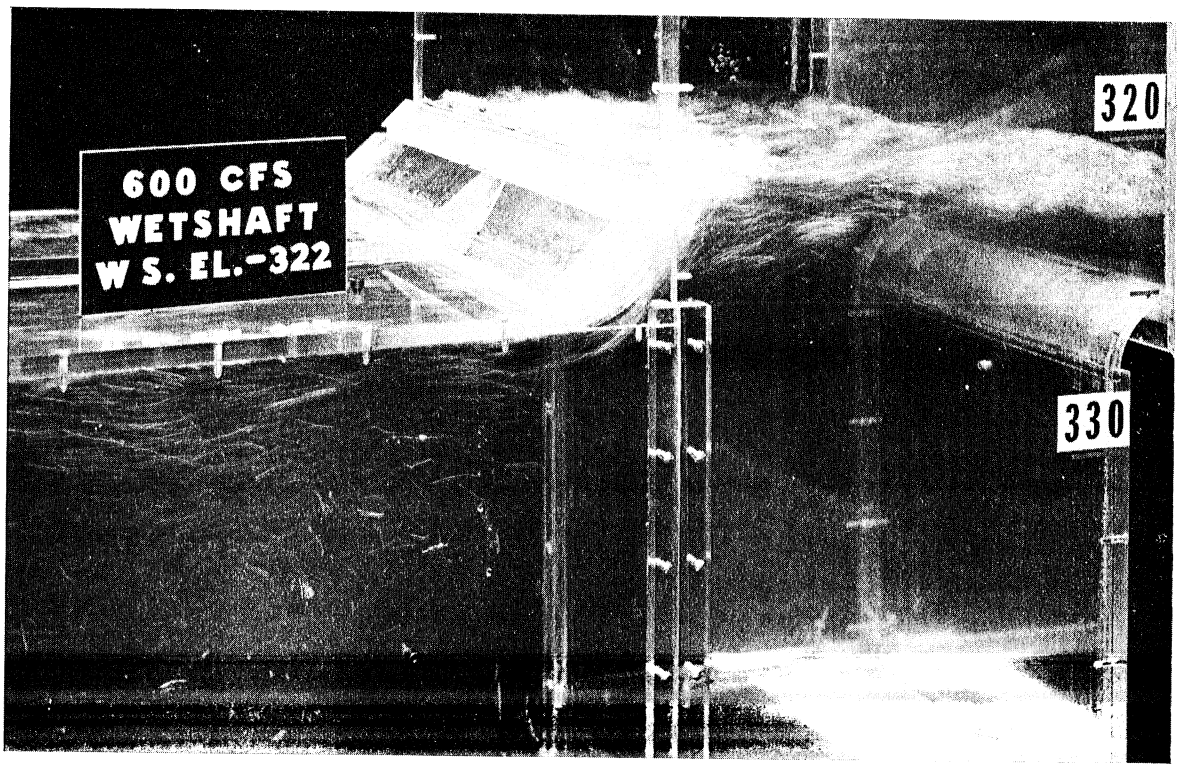

Fig. 34 - Air Entrainment and Free Surface Configuration in Drop Structure at Low Stage. Design B.

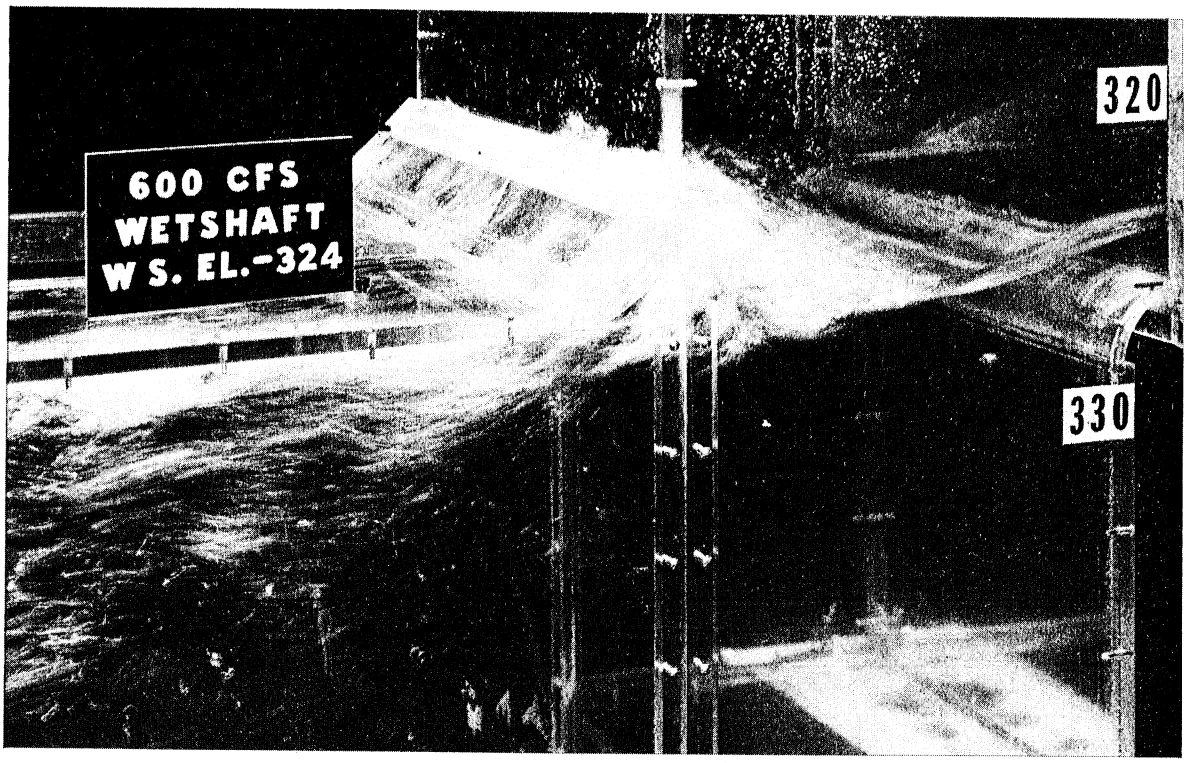

Fig. 35 - Air Entrainment and Free Surface Configuration in Drop Structure at Low Stage. Design B.

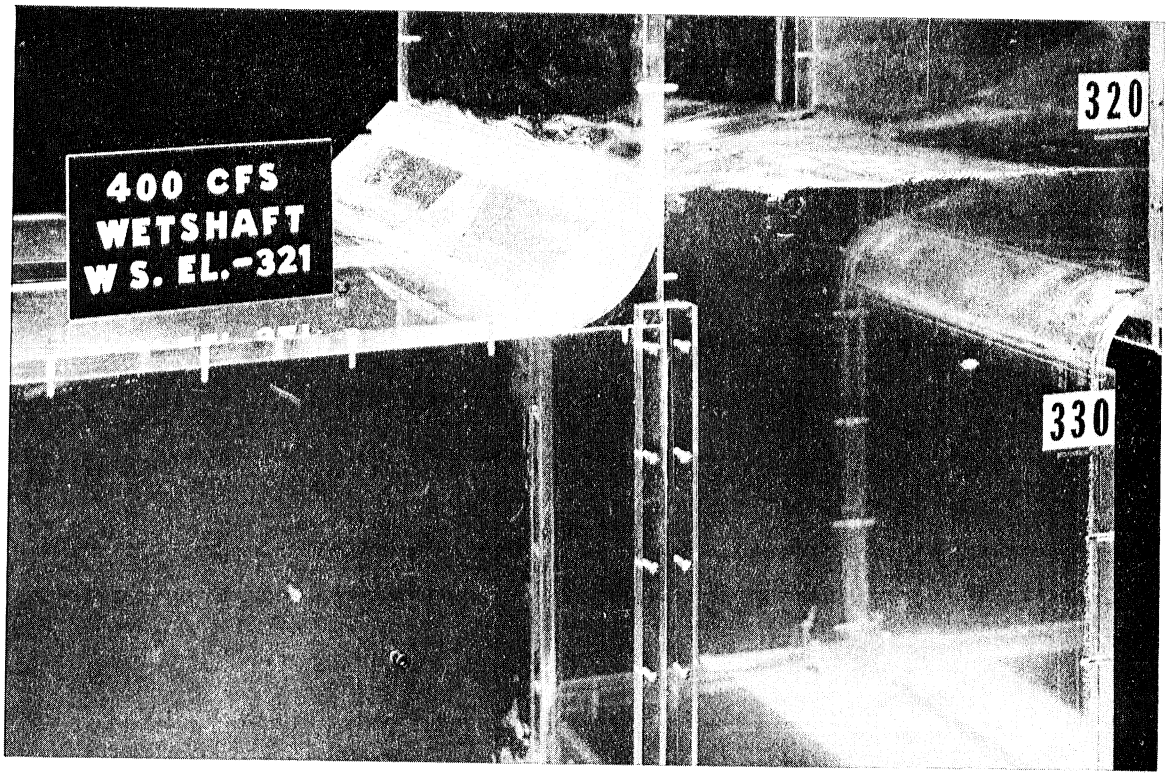

Fig. 36 - Free Surface Configuration in Drop Structure at Low Stage. Design B.

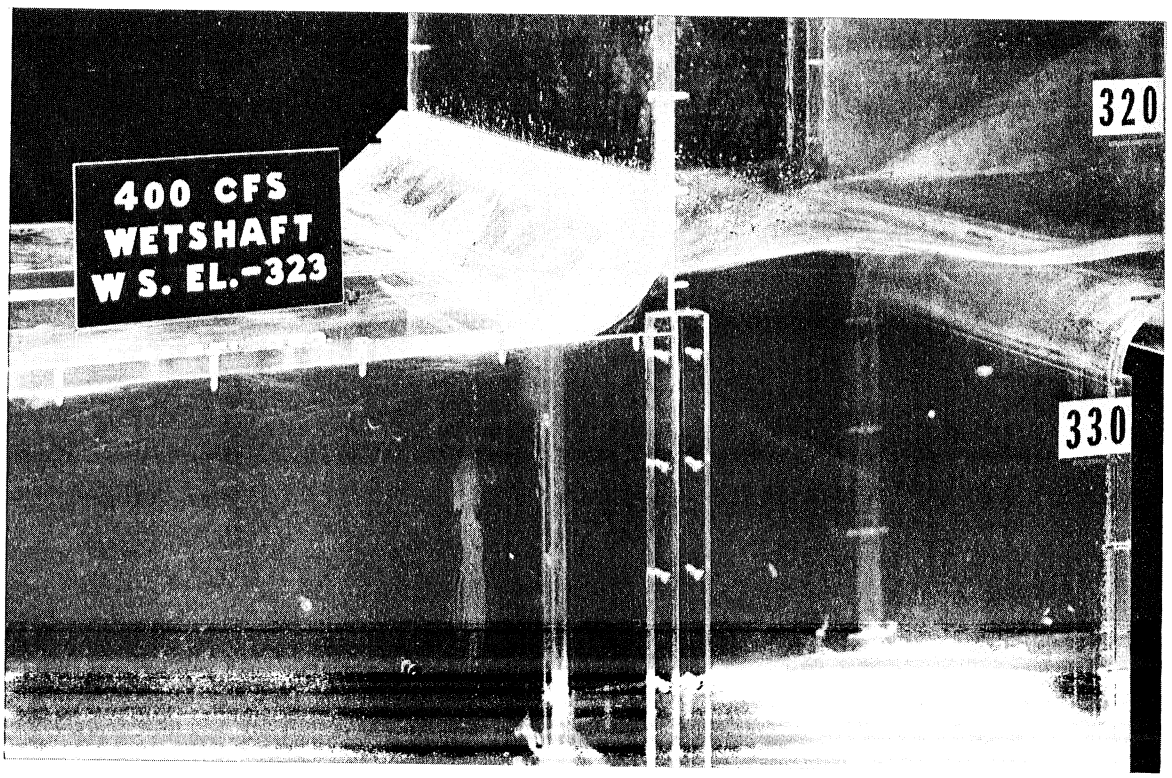

Fig. 37 - Air Entrainment and Free Surface Configuration in Drop Structure at Low Stage. Design B.

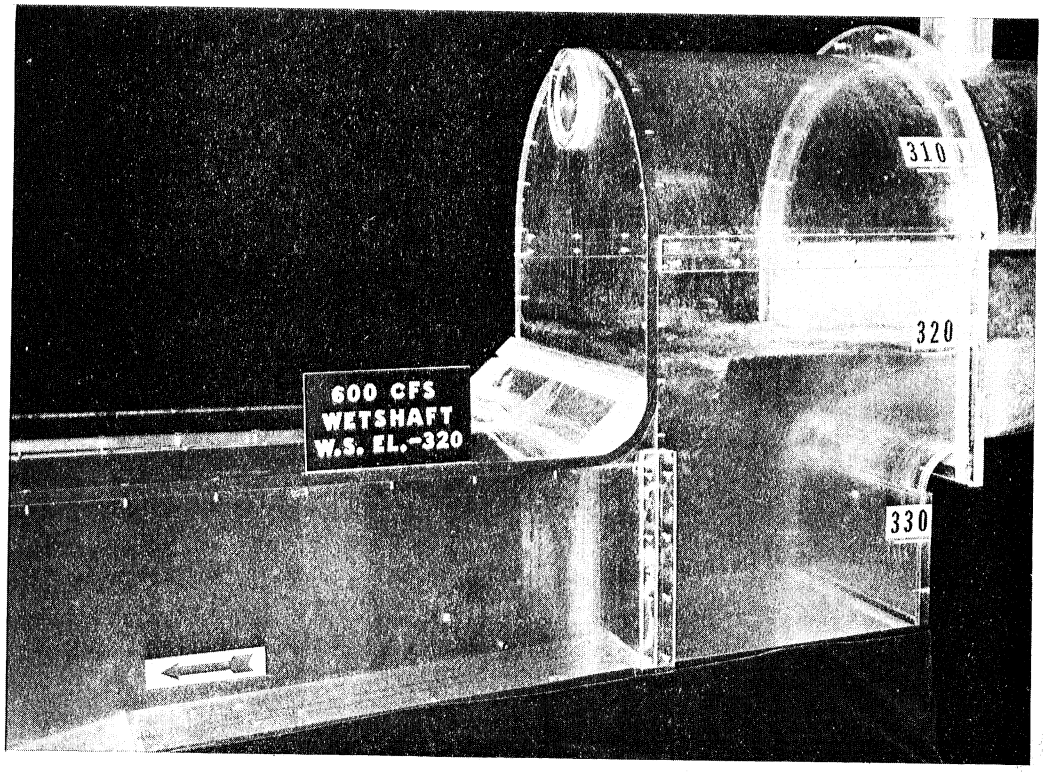

Fig. 38 - Free Surface Configuration and Vortex Formation in Drop Structure at Low Stage. Design C.

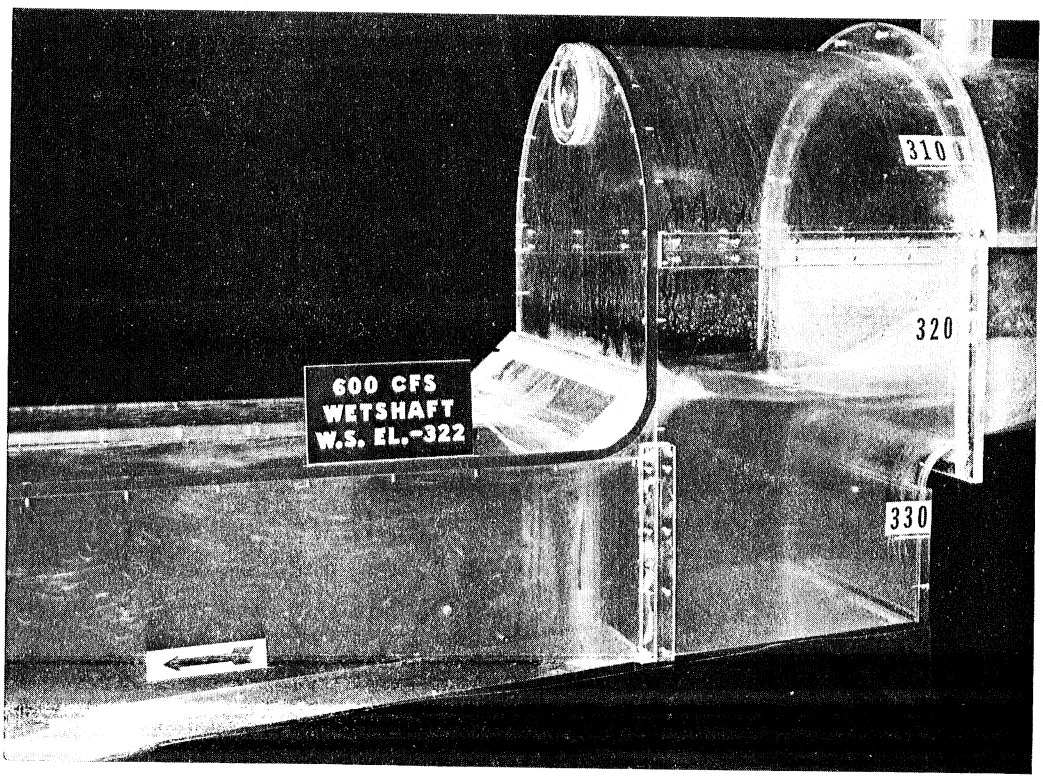

Fig. 39 - Incipient Air Entrainment and Surface Configuration in Drop Structure at Low Stage. Design C.

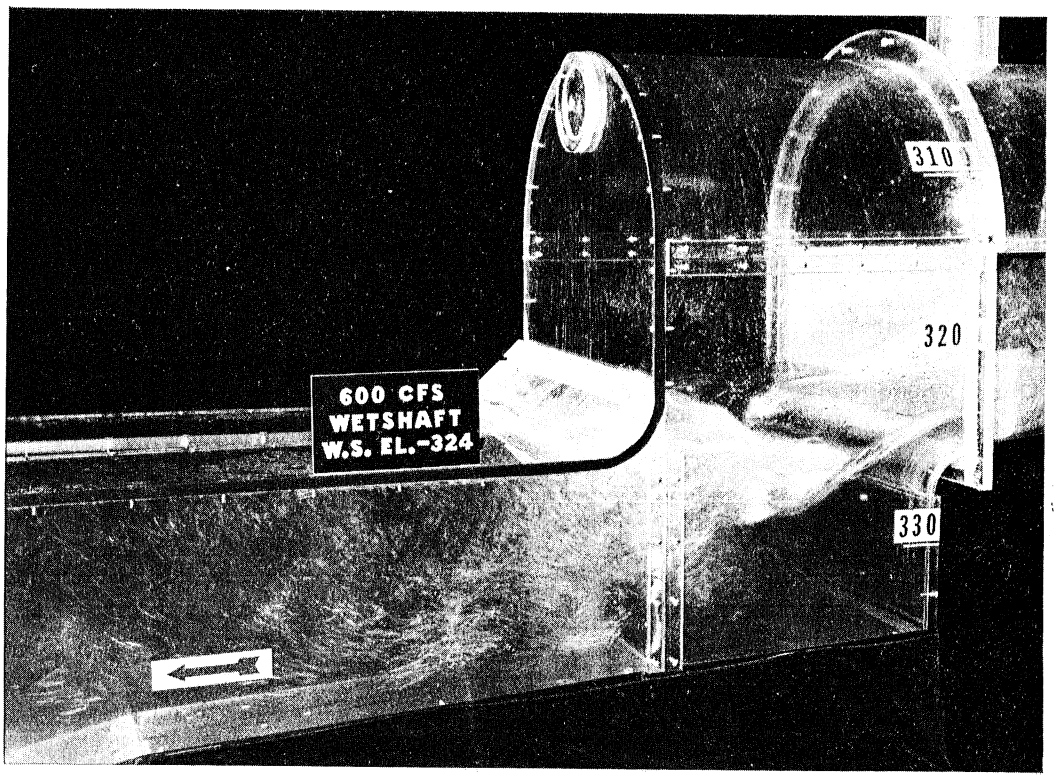

Fig. 40 - Air Entrainment and Free Surface Configuration in Drop Structure at Low Stage. Design C.

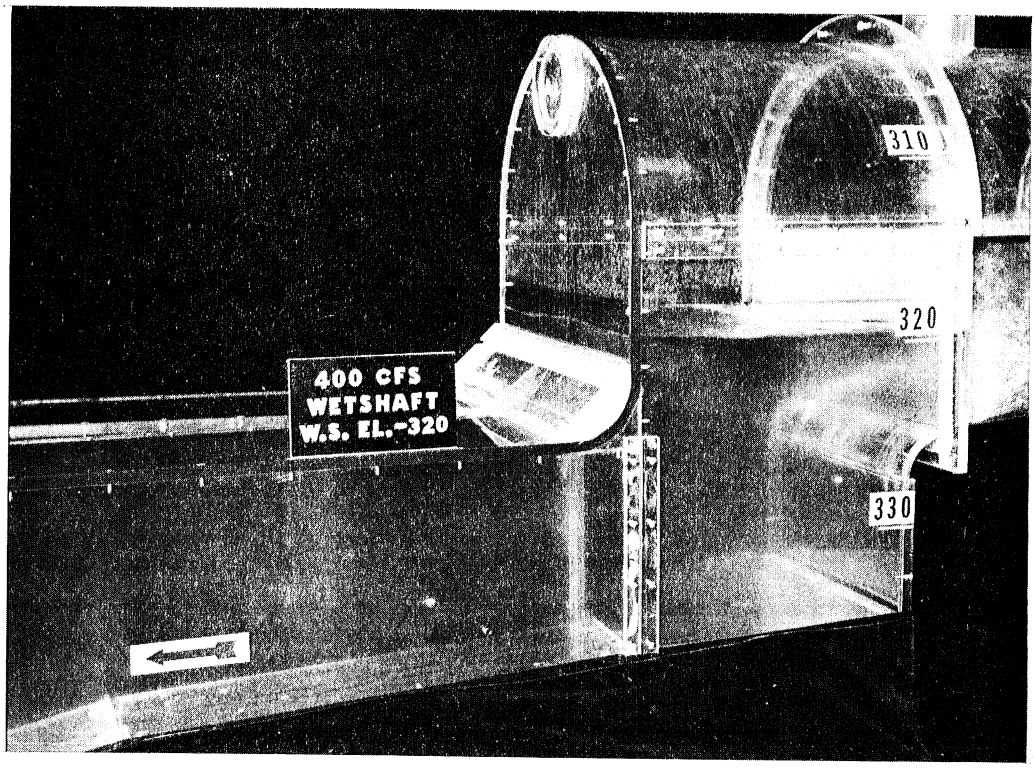

Fig. 41 - Free Surface Configuration and Vortex Formation in Drop Structure at Low Stage. Design C.

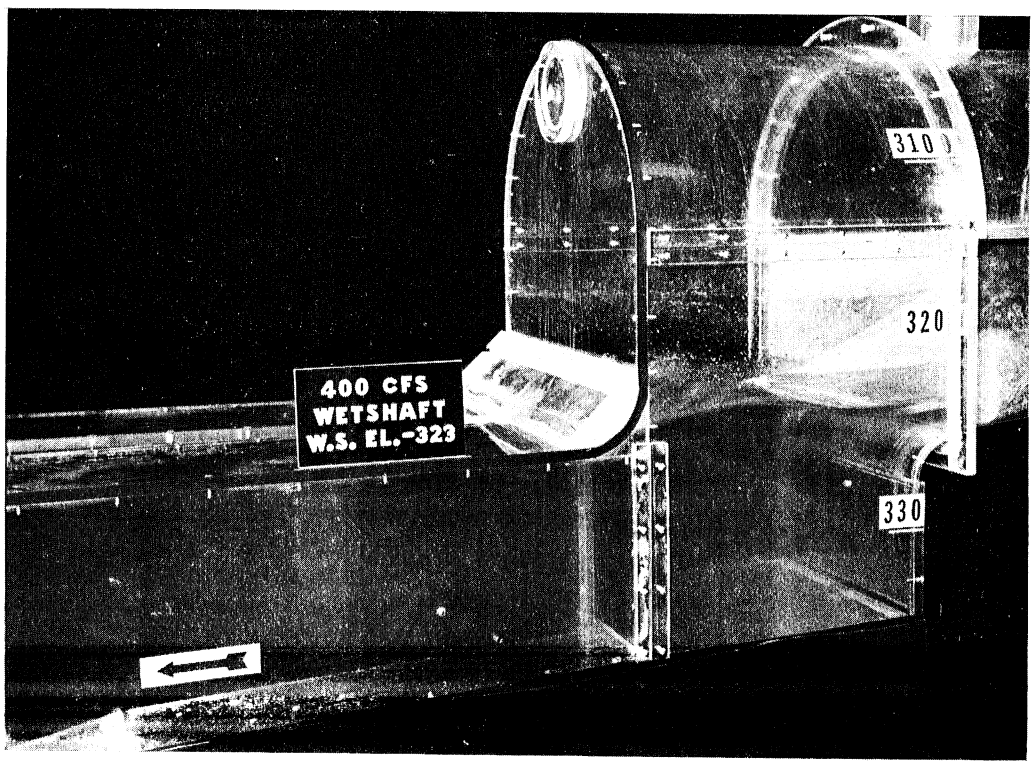

Fig. 42 - Incipient Air Entrainment and Surface Configuration in Drop Structure at Low Stage. Design C.

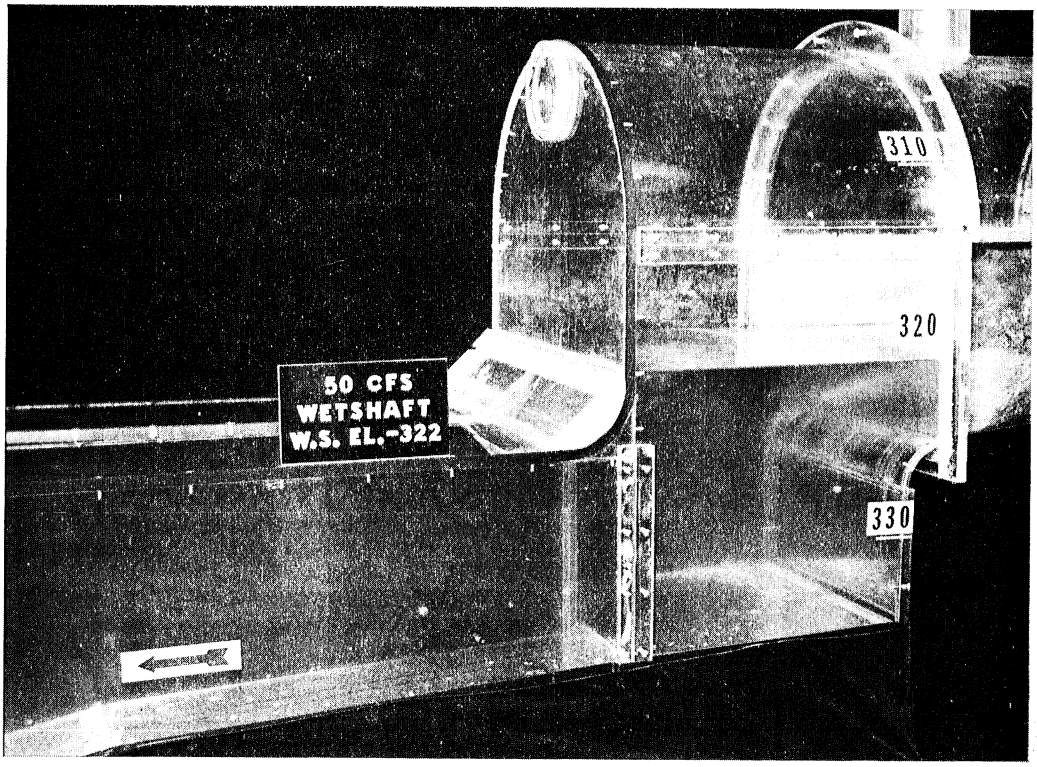

Fig. 43 - Free Surface Configuration and Vortex Formation in Drop Structure at Low Stage and Very Low Flow. Design C.

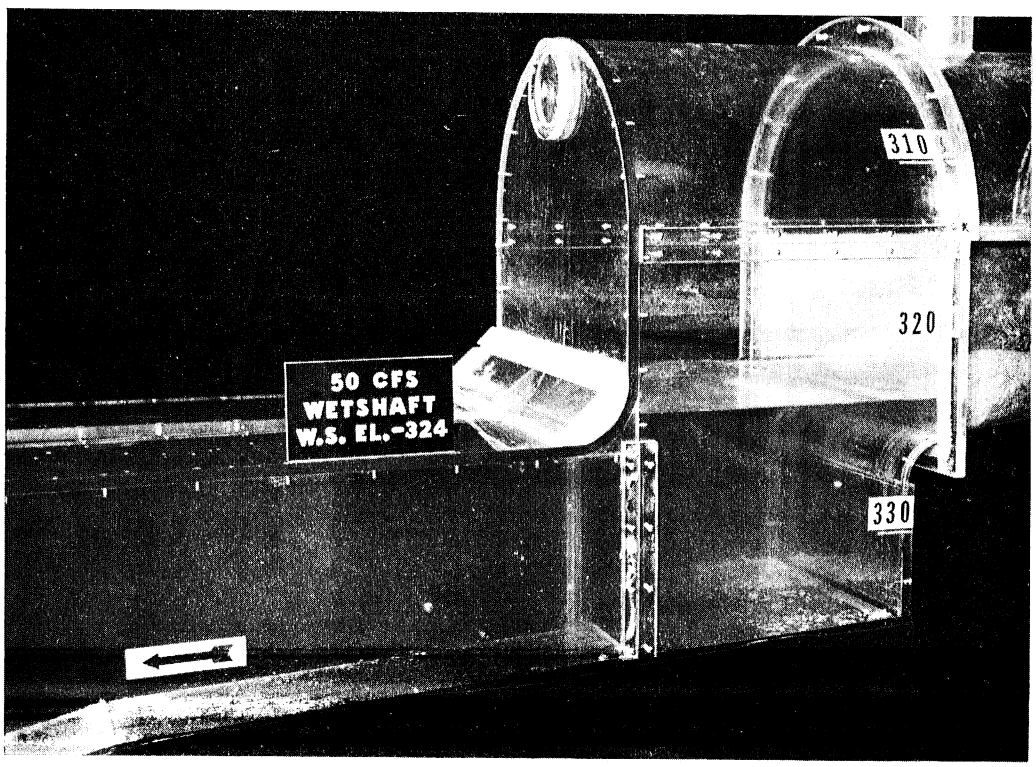

Fig. 44 - Free Surface Configuration and Vortex Formation in Drop Structure at Low Stage and Very Low Flow. Design C.

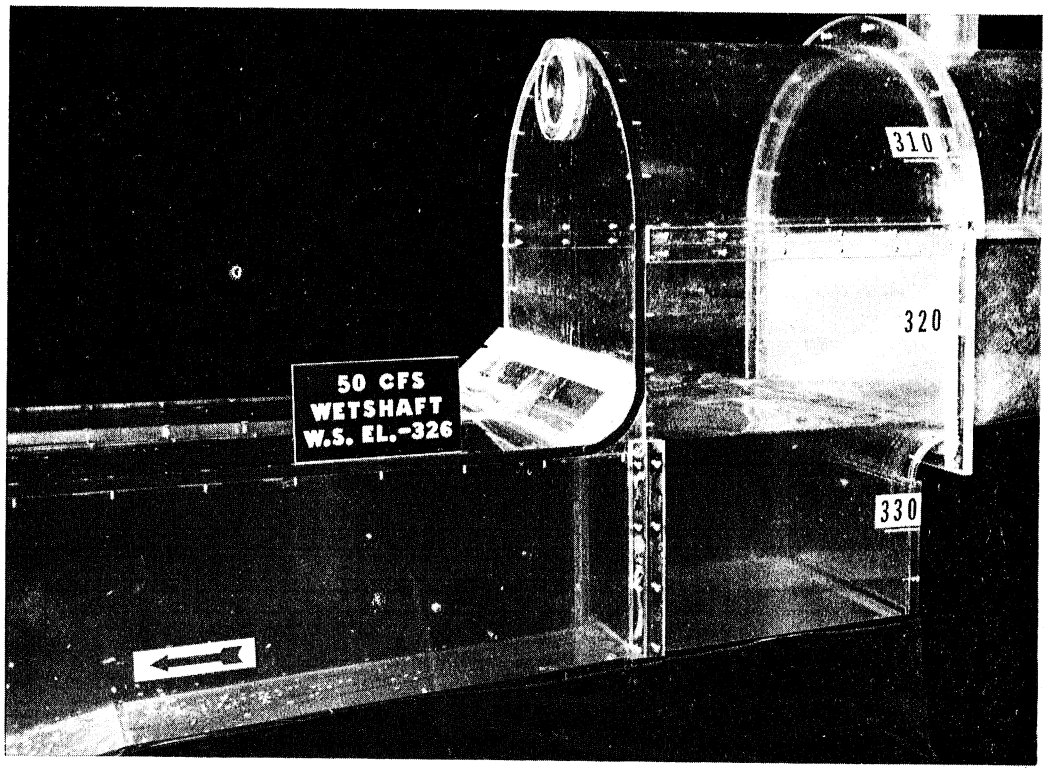

Fig. 45 - Free Surface Configuration and Vortex Formation in Drop Structure at Low Stage and Very Low Flow. Design C.

3. Piezometric Heads and Head Losses

3.1. Suction Header

The following piezometric heads and the following head losses were determined from measurements on the 1:14 scale model of the suction header with a total pumping rate of 280 cfs (pump 1: 50 cfs; pumps 2 and 3: 115 cfs, each) and at a wet shaft water elevation of -322.0:

Station	Flow Rate (cfs)	Elevation of Piezometric Gradeline (ft)	Head loss Between Wet Shaft and Indicated Station (ft)
1	115	-326.0	1.6 ± 0.4
2	115	-323.4	1.1 ± 0.2
3	115	-322.8	0.8 ± 0.2
4	115	-325.9	1.4 ± 0.6
5	115	-323.3	1.0 ± 0.2
6	230	-323.1	0.7 ± 0.2
7	50	-327.9	3.0 ± 0.9
8	50	-323.5	1.5 ± 0.2
9	280	-323.4	0.8 ± 0.2
10	280	-323.1	0.3 ± 0.2
wet shaft	280	-322.0	0

The standard error based on independent experiments is given next to the head loss figure. With the possible exception of the gate valves*, head losses determined in the model will closely represent those in the prototype. For verification, measurements of piezometric heads in the suction header and computations of head losses between each of stations 1 through 11 in Fig. 46 and the wet shaft at 280 cfs flow rate per suction header were made at different main suction header Reynolds numbers with the following results:

---

*i.e., losses between Stations 1 and 2, 4 and 5, and 7 and 8. (See Appendix for explanation.)

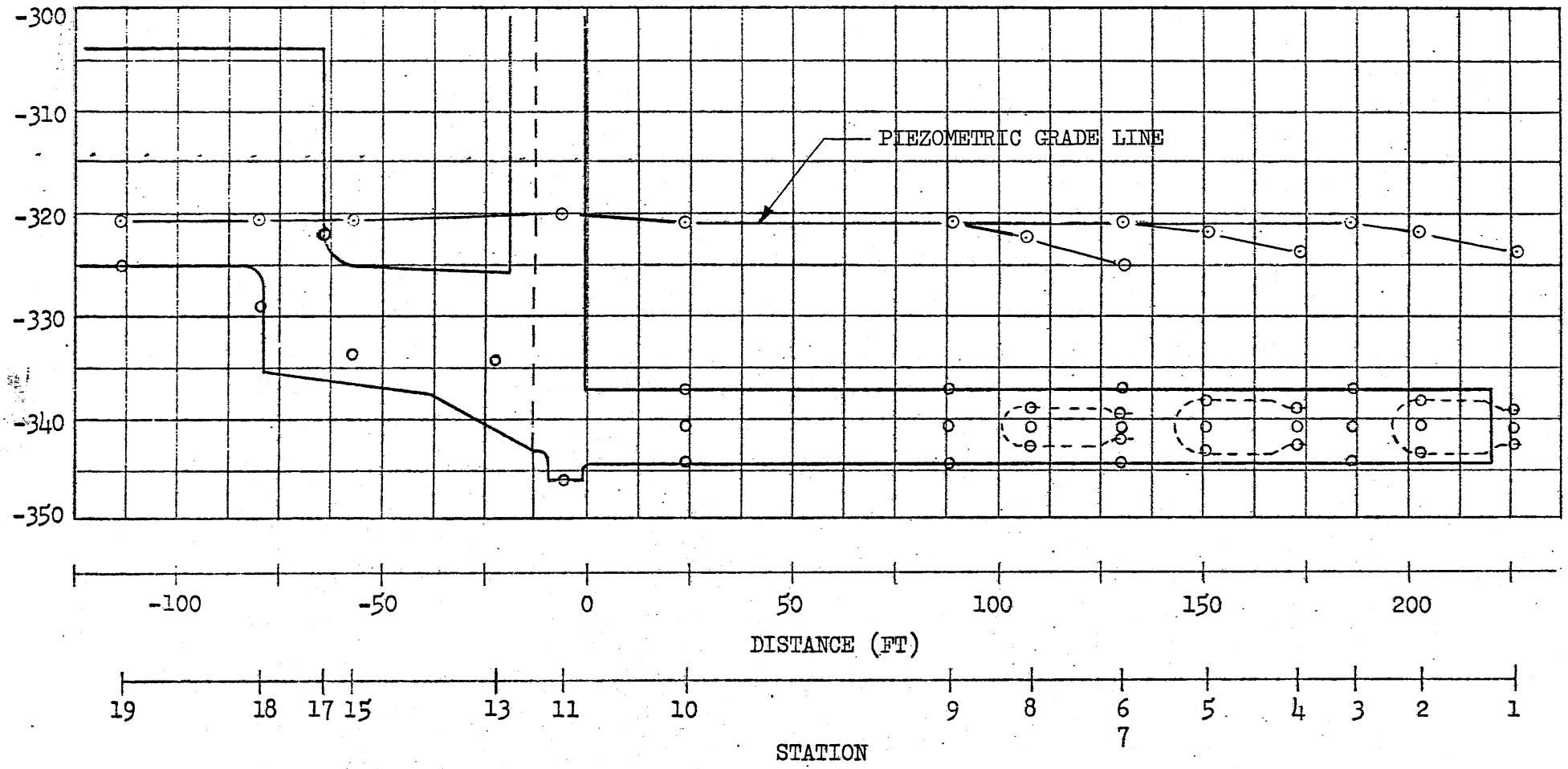

Fig. 46 - Piezometric Grade Line at Total Flow of 600 cfs and Wet Shaft Water Surface Elevation -320. Design C.

Station	Flow Rate (cfs)	Re = 58,500 Head Loss (ft)	Re = 115,000 Head Loss (ft)	Re = 150,500 Head Loss (ft)	Re = 217,000 Head Loss (ft)
1	115	1.6	1.5	2.2	2.1
2	115	1.1	0.9	1.3	1.2
3	115	0.8	0.7	0.8	0.7
4	115	1.4	1.3	2.4	2.2
5	115	1.0	0.9	1.2	1.1
6	230	0.8	0.5	0.8	0.7
7	50	3.0	2.2	1.6	1.7
8	50	1.5	1.0	1.3	1.3
9	280	0.8	0.5	0.8	0.7
10	280	0.3	0.2	0.4	0.5
wet shaft	280	0	0	0	0

With the exception of the stations representing the intakes of the pumps (Stations 1, 4, and 7) results are quite consistent over the Reynolds number range.

Reynolds numbers in the model were varied by changing flow rates or water temperatures. Head losses were then reduced to those for the design flow by multiplication with the square of the flow ratios, implying that head losses are proportional to the square of the mean flow velocities. Differences shown in the table above are minor and with few exceptions within the error of the piezometric head readings on a laboratory manometer board, including the effects of some turbulent transients.

The data on head losses obtained in the model do not show any strong trend in head losses as a function of Reynolds number. It is therefore expected that the prototype which will operate at Reynolds numbers above two million at full pumping rate will experience head losses of the same magnitude as given above.

The head loss attributable to wall friction along the total length of the suction header is less than 0.2 ft (see Appendix).

The head losses and the configuration of the piezometric grade line did not change appreciably with wet shaft water surface elevation as shown in Fig. 46, 47, and 48.

3.2 Divided Duct, Box Drop Structure

Head losses in those parts of the structure are quite small. They are expressed in the following table for a total pumping rate of 560 cfs and at a wet shaft water elevation of -322.0 for Design C.

Station	Flow Rate (cfs)	Elevation of Piezometric Gradeline (ft)	Head Loss Between Indicated Station and Wet Shaft (ft)
11	280	0	0
13	280	-322.0	0.1
15	280	-321.8	0.2
17	560	-321.5	0.5
18	560	-321.8	1.8
19	560	-321.3	3.7

In the transition from the Calumet tunnel to the box drop structure the flow becomes supercritical when the wet shaft water surface elevation becomes low as shown e.g. in Figs. 39 and 42. The head losses in the drop structure and the Calumet Tunnel approach are strongly dependent on differences in flow velocities produced by differences in stages. Measured head losses between Station 19 in the tunnel, shown in Fig. 46, and the wet shaft are given below for total flows of 560 cfs and different stages.

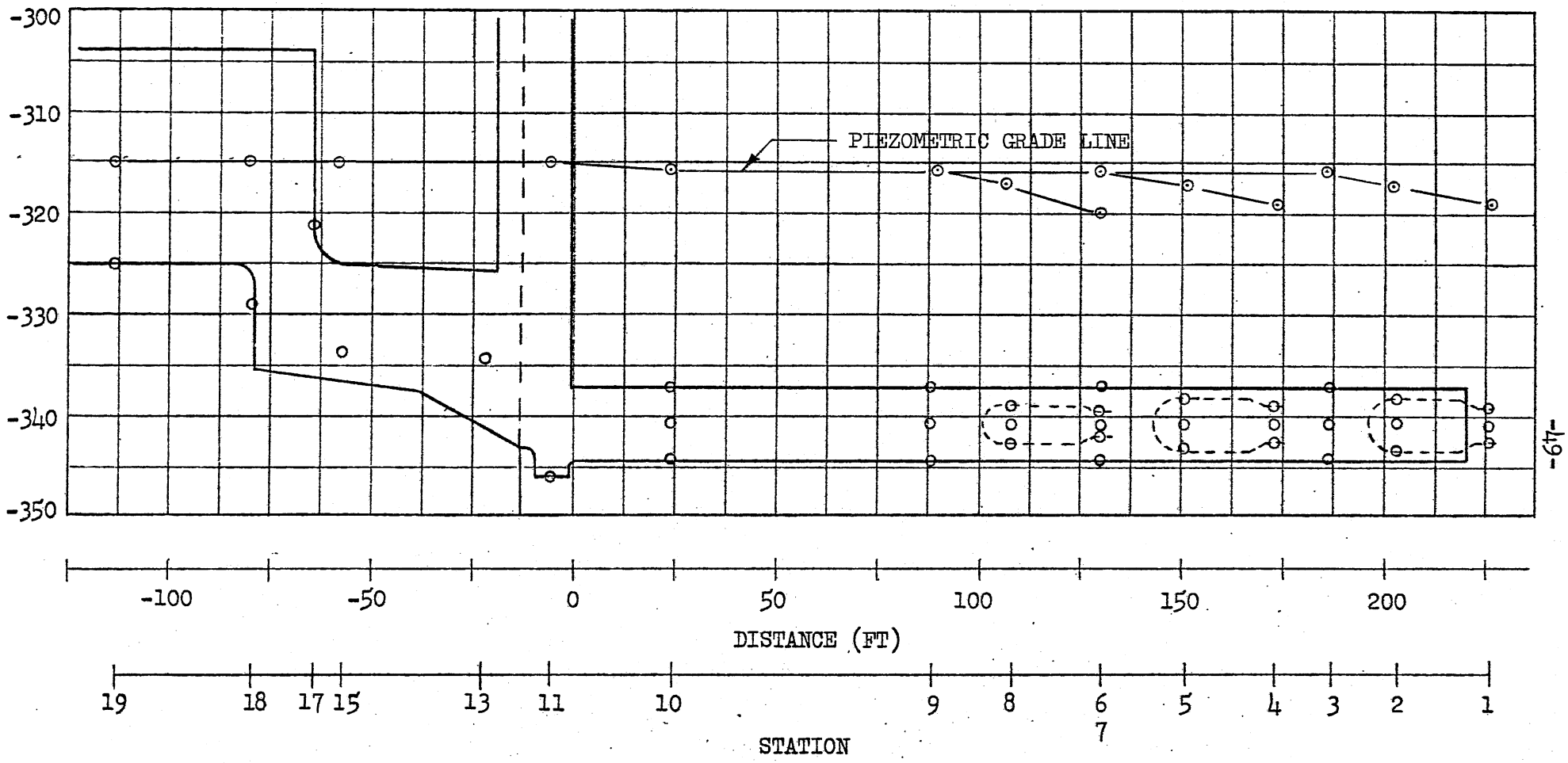

Fig. 47 - Piezometric Grade Line at Total Flow of 600 cfs and Wet Shaft Water Surface Elevation -315. Design C.

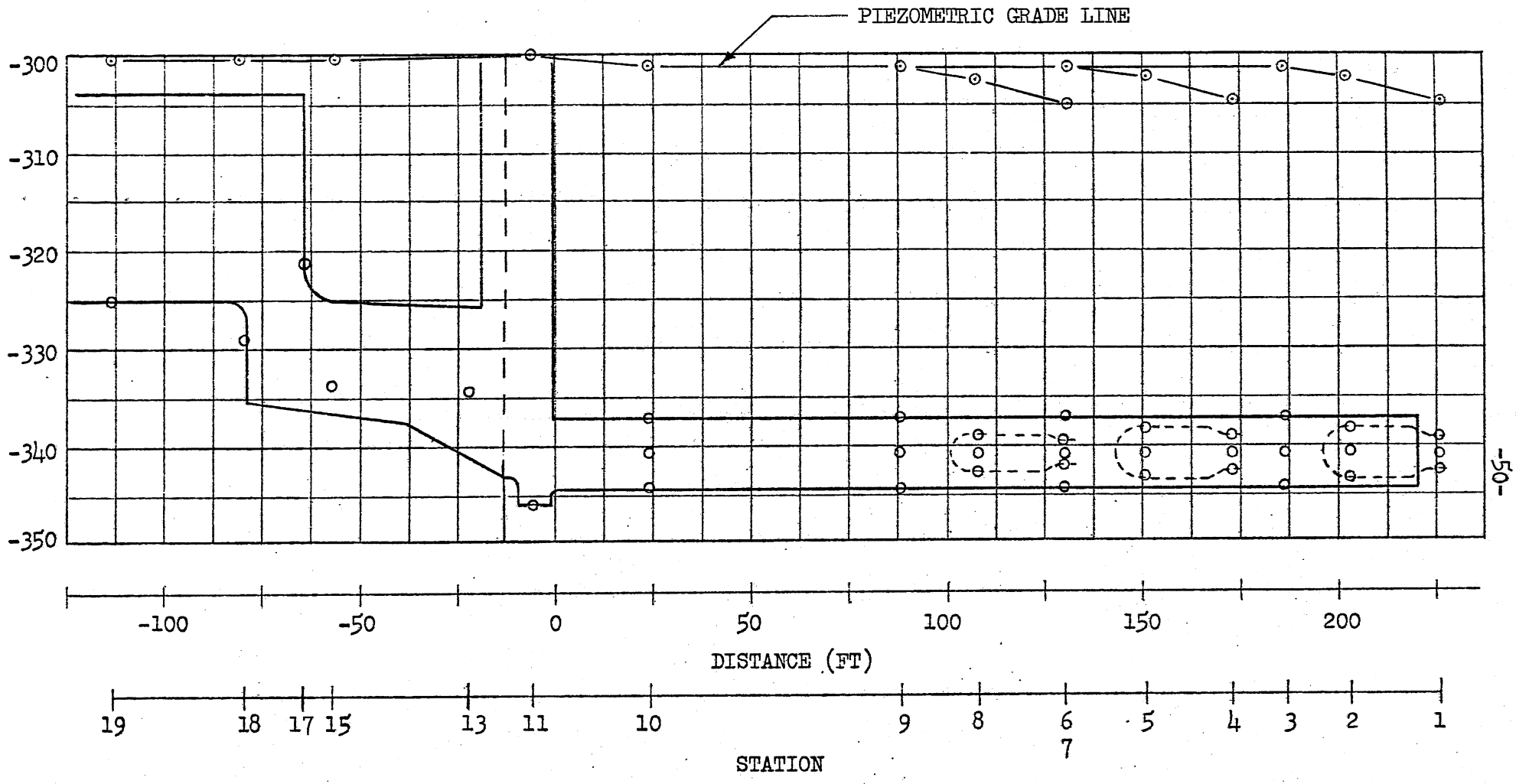

Fig. 48 - Piezometric Grade Line at Total Flow of 600 cfs and Wet Shaft Water Surface Elevation -300. Design C.

Wet Shaft W.S. El. (ft)	Head Loss (ft)
-325	7.1
-322	3.7
-318	0.4
-315	0.2
-300	0.1

3.3. Bar Screen

The vertical bars of the screen are 3.5 in. x 0.5 in. with the longer dimension in flow direction. The opening between bars is 3.0 in. The bar screen is supported by horizontal channels (12 in. x 3 in.) spaced vertically at 5 ft intervals. The open part of the bar screen extends from elevation -343 to approximately -298. At a wet shaft water surface elevation of -322, the exposed bar screen area is therefore 21 x 9 ft or 189 ft^2 of which 162 ft^2 are open to the water. The bars are rectangular in shape. The Reynolds number of the flow between bars at a pumping rate of 560 cfs and at 40°F (280 cfs per screen) will be approximately 26,000 in the prototype and is approximately 500 in the model. If the flow were a duct or pipe flow this would result in an undesirable laminar flow condition in the model. However, because the distance of travel through the bar screen is only very short and because the streamlines through the bar are not rectlinear, the turbulent flow upstream from the screen will also be carried through the bar screen in the model.

Observed head losses through the bar screen at wet shaft W.S. El. -320 and a total pumping rate of 560 cfs (280 cfs per screen) were as follows:

clear rake (no debris)	not measurable
approximately 25 percent of surface area randomly obstructed	not measurable
approximately 50 percent of surface area randomly obstructed	0.5 ft
approximately 70 percent of surface area randomly obstructed	1.1 ft
approximately 85 percent of surface area randomly obstructed	2.6 ft

Most of the head loss was absorbed by a decrease in water surface elevation (below -320) downstream from the screen. The increase in water surface elevation upstream from the rake did not exceed 0.4 ft.

4. Entrainment of Liquid Floating Materials (Hydrocarbons, etc.)

In the event of an accidental fuel or oil spill, hydrocarbons may flow into the storm sewer system. If these materials are not removed, the danger of an underground explosion exists. Experiments were therefore conducted to determine if and how such materials would flow through the system. Kerosene (specific gravity 0.82) in quantities of 2 gallons - representing a prototype spill of 5,500 gallons - was introduced into the head box of the model. The following observations were made:

Floating at the water surface the material reached the box drop structure where it was dispersed into drops of sizes up to about one half inch. In the divided duct many of the drops coagulated and rose for the most part to the crown of the duct. They were subsequently entrained into the wet shaft where they accumulated as a layer of 1 to 2 ft thickness on the water surface. At wet shaft water surface elevations near -320 or -322 the layer is very stable and no entrainment into the suction header occurs.

Subsequently, a drawdown of the water in the wet shaft was tested. A closed gate at the upstream end of the wet shaft was simulated by installing a plate between wet shaft and duct. Pump No. 1 was operated at a rate near 10 cfs. No entrainment of kerosene into the suction header occurred until the kerosene reached the crown of the suction header. It then spread into and over the total length of the suction header quickly followed by air. Some of the oil was drawn into the pump as the oil layer reached the crown of the branch header. However, pumping had to be stopped to prevent air entrainment by the pump. A residual oil layer remained.

The system was subsequently slowly filled with water, the gate was removed. Residual oil from the suction header flowed back into the wet shaft under its own buoyancy. A residual layer 0.5 to 1 ft thick remained in the wet shaft.

It can be concluded from this experiment that in the case of an oil spill,

(a) the oil will accumulate in the wet shaft,

(b) under normal operation it will not be entrained beyond the wet shaft unless the bottom of the oil layer reaches the crown of the suction header intake,

(c) a drawdown of the water surface in the wet shaft will entrain much of the oil with the water into pump No. 1, but a residual layer will nevertheless remain in the wet shaft.

5. Entrainment and Deposition of Sand and Gravel (Grit)

Grit (sand) is carried in almost all sewer systems. Experiments were therefore conducted to examine how such materials move through the system. The model grit was a natural sand with the size distribution shown in

Figure 49. It simulates a coarse sand to fine gravel in the prototype.

The sand was introduced into the Calumet tunnel at the upstream end of the model through the head box. Only at low stages would the flow in the tunnel transport the material. At the end of the tunnel the grit would fall into the drop structure and accumulate as shown in Figs. 50 and 51. Typically, sediment was fed into the model over a 30 to 60 minute period in amounts of up to 2 ft^3, representing up to 200 cubic yards of gravel. As time progressed, sediment was carried downstream in the duct. In the original design configuration (Design A) the tendency for sediment to permanently deposit in the divided duct was observed to be small, because of the high level of turbulence produced by the flow in the drop structure. The modification of the drop structure to Design B had a very marked effect on the sediment (grit) deposit. Bed configurations in Design B after approximately 5 hours of experimental time (representing about 18 hours prototype time) and after approximately 16.5 hours of experimental time (representing about 2.5 days in the prototype) are shown in Figs. 52 and 53, respectively.

It was found that even after 16.5 hours of continuous flow in the model at an equivalent value of 600 cfs a complete steady-state had not been reached as minute amounts of sand were still entering the suction header. Decreasing the flow rate to single pump operation at 115 cfs made the bed absolutely motionless. Also, after the Calumet tunnel was filled to wet shaft elevation -300 and after pumping was resumed at 600 cfs, the bed configuration was not appreciably altered in the following two hours. Sand motion was barely noticeable.

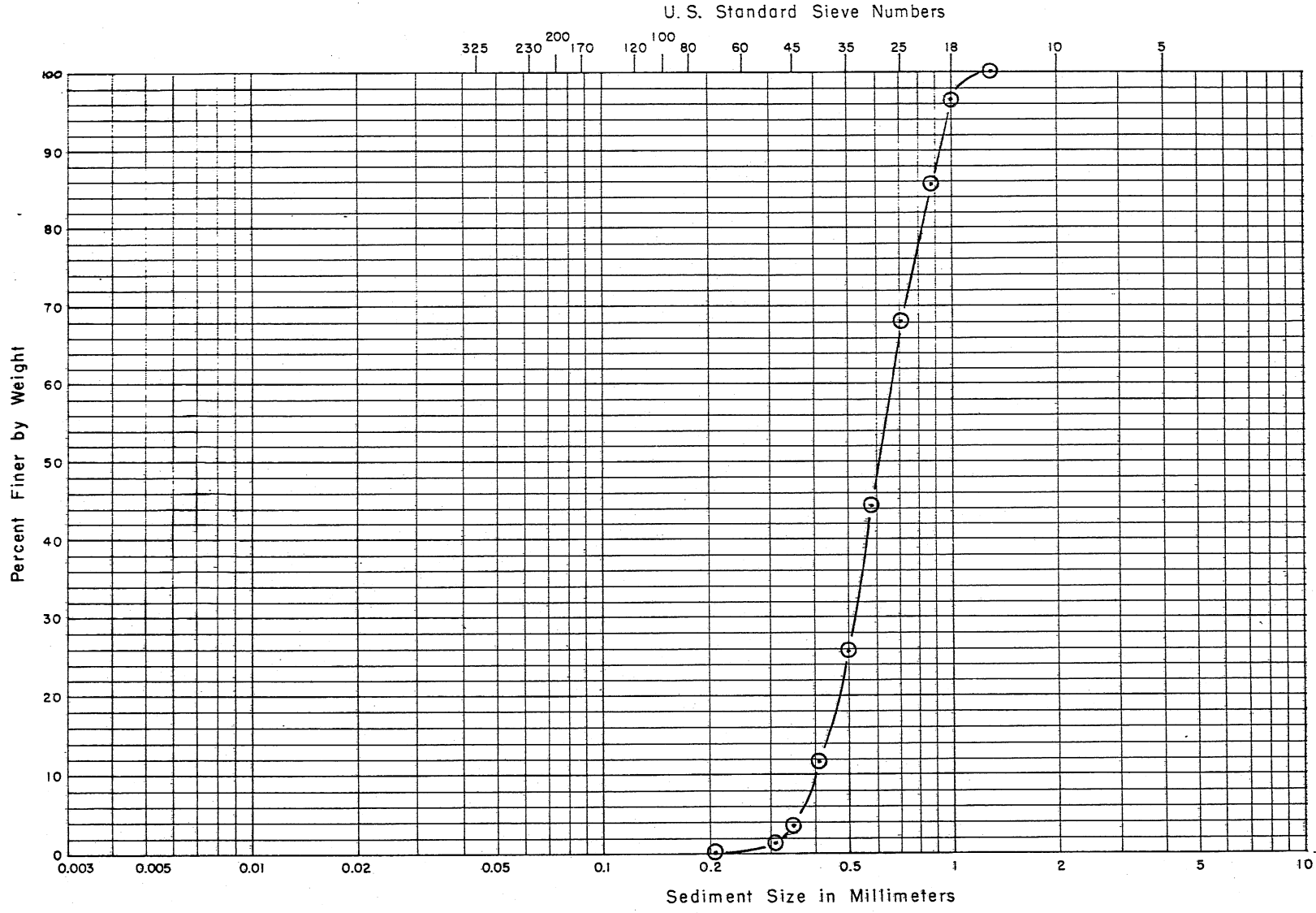

Fig. 49 - Size Distribution of Model Sand used in Grit Transport Experiments

For practical purposes the bed configuration shown in Fig. 53 was considered an equilibrium bed configuration.

In order to reduce the sizeable volume of deposited material it was decided to raise the invert of the divided duct resulting in Design C shown in Fig. 10.

The grit transport experiment was repeated for Design C at 600 cfs flow and wet shaft water surface elevation -320. A total of 1.4 ft^3 of material was introduced over a period of half an hour. This would simulate roughly 143 cubic yeards of material arriving at the structure over a period of roughly 1.9 hours or a prototype volumetric grit inflow rate of 0.56 cfs. The observed sequence of scour and deposition patterns within the structure is shown in Figs. 54 through 64. The last pictures are taken at 1 hour intervals in the model. No major permanent deposition in the drop structure occurred. There was a permanent or nearly permanent deposition upstream from the bar screen and underneath the gate structure. The total amount of material remaining in the structure after approximately 1.5 prototype days was about 40 cubic yeards divided equally between the two ducts. Compared to the conditions observed in the previous design the total volume of grit deposit in the structure was much reduced.

A reduction of the width of the duct downstream from the invert break point would probably prevent permanent grit deposit completely. To test this idea a preliminary experiment with semi-circular flow restricters placed on the walls of the duct was conducted. The restricters had a radius of $r = 1.5$ ft and were chosen because they could be easily installed. Other geometries may be preferable. The restricters were placed on each wall of the duct, 3 ft upstream and downstream from the influent gate slot. The

effect of the restricters was to increase flow velocities and turbulence in the region, where potential grit deposition occurred previously. Scouring of temporary deposits was complete and permanent deposition of the model grit was prevented. The results of these grit experiments, as all previous ones, are qualitative but show the potential benefits of a further improved design.

It was also observed at the end of the experiment that a small amount of grit covered the bottom of the pump sump in the wet shaft. The total accumulation was, however, barely measurable. A reduction of the flow to 115 cfs (one pump operation, as well as operation at wet shaft W.S. El. -300 (full tunnel) at 600 cfs total pumping rate for an hour did not change the sand deposit appreciably.

Grit deposition in the suction header is possible temporarily. With low input of grit, the suction header is cleared from upstream to downstream. Permanent deposition was observed only in the dead end of the pipe downstream from branch header outlet No. 3. The volume of deposit was quite small and was found to be on the order of 0.1 ft^3 after approximately 2 ft^3 of grit had moved through the system.

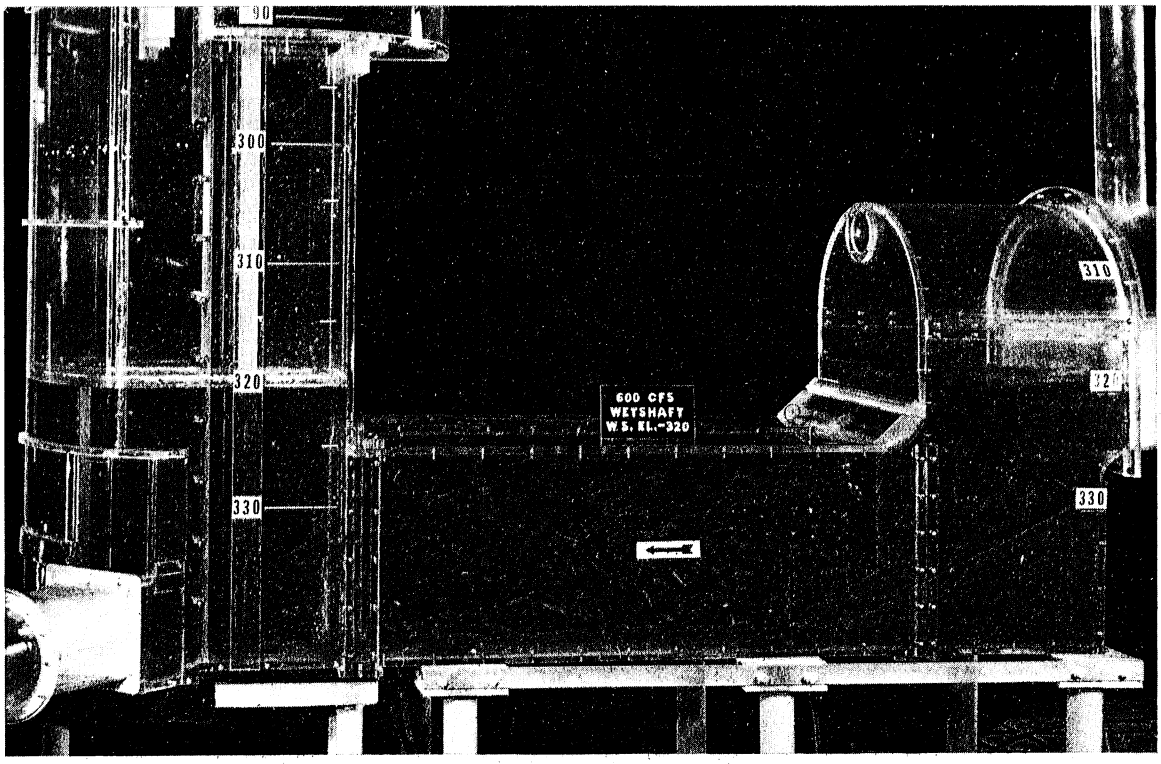

Fig. 50 - Early Stages of Grit Transport through Drop Structure and Divided Duct. Design B.

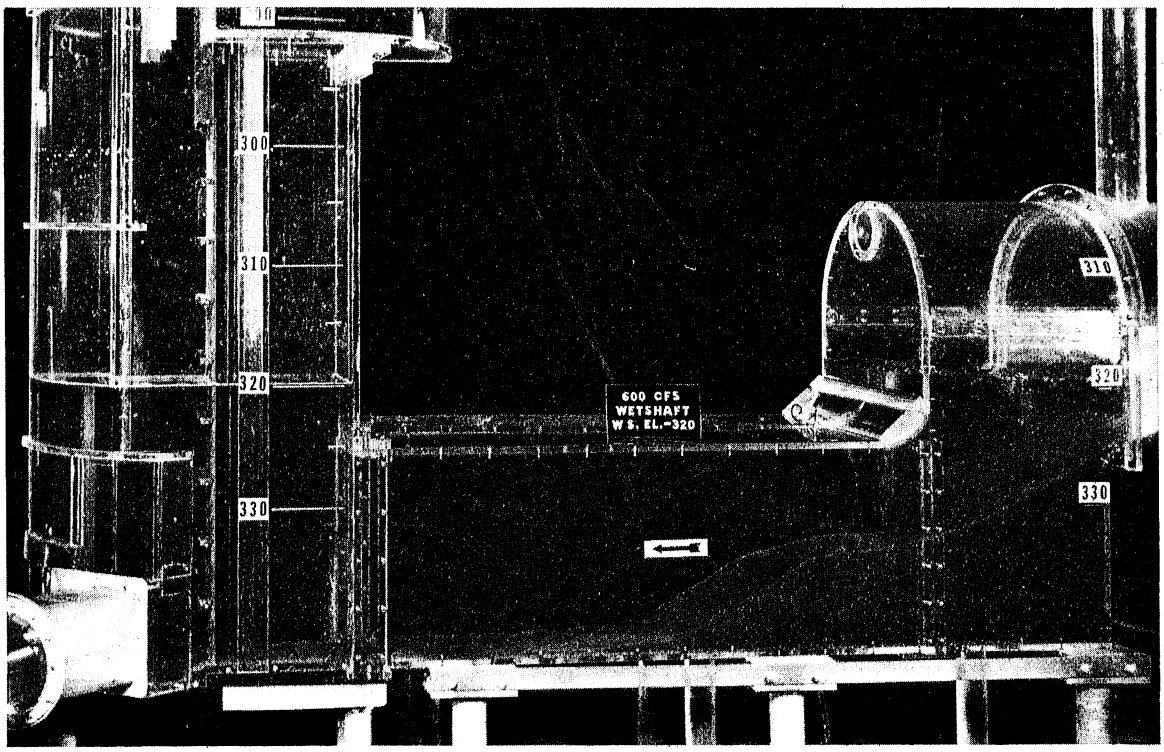

Fig. 51 - Early Stages of Grit Transport through Drop Structure and Divided Duct. Design B.

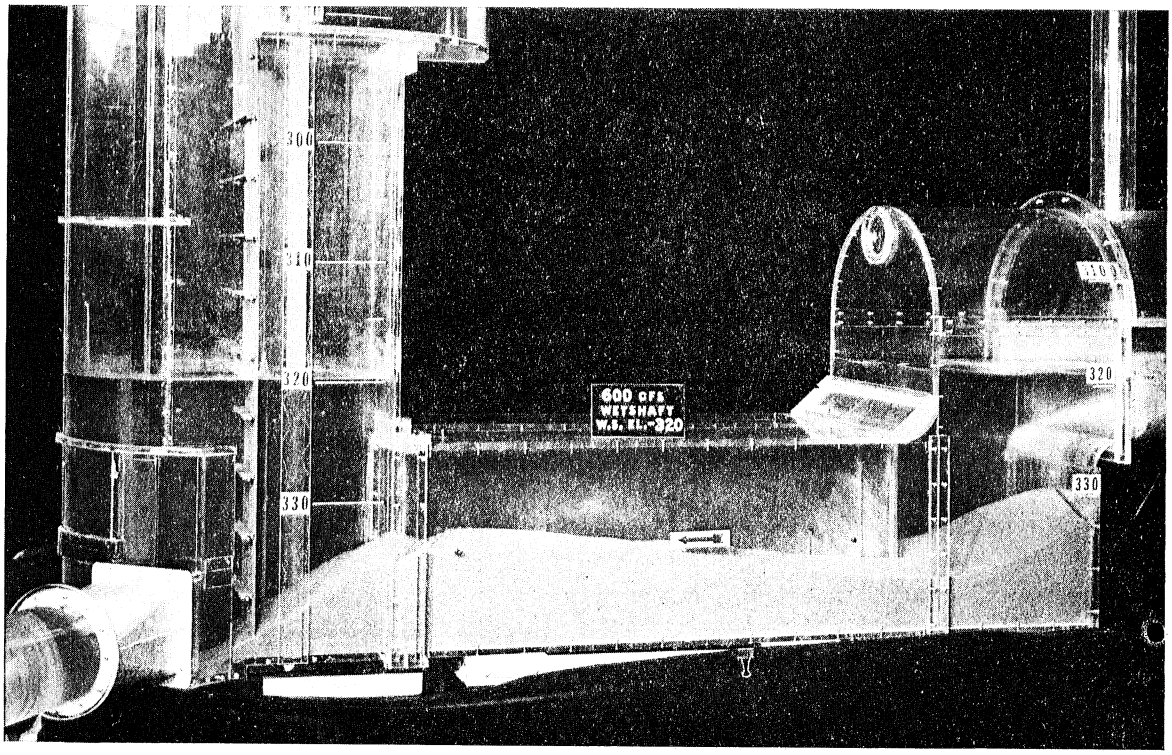

Fig. 52 - Final Stages of Grit Transport through Drop Structure and Divided Duct. Design B.

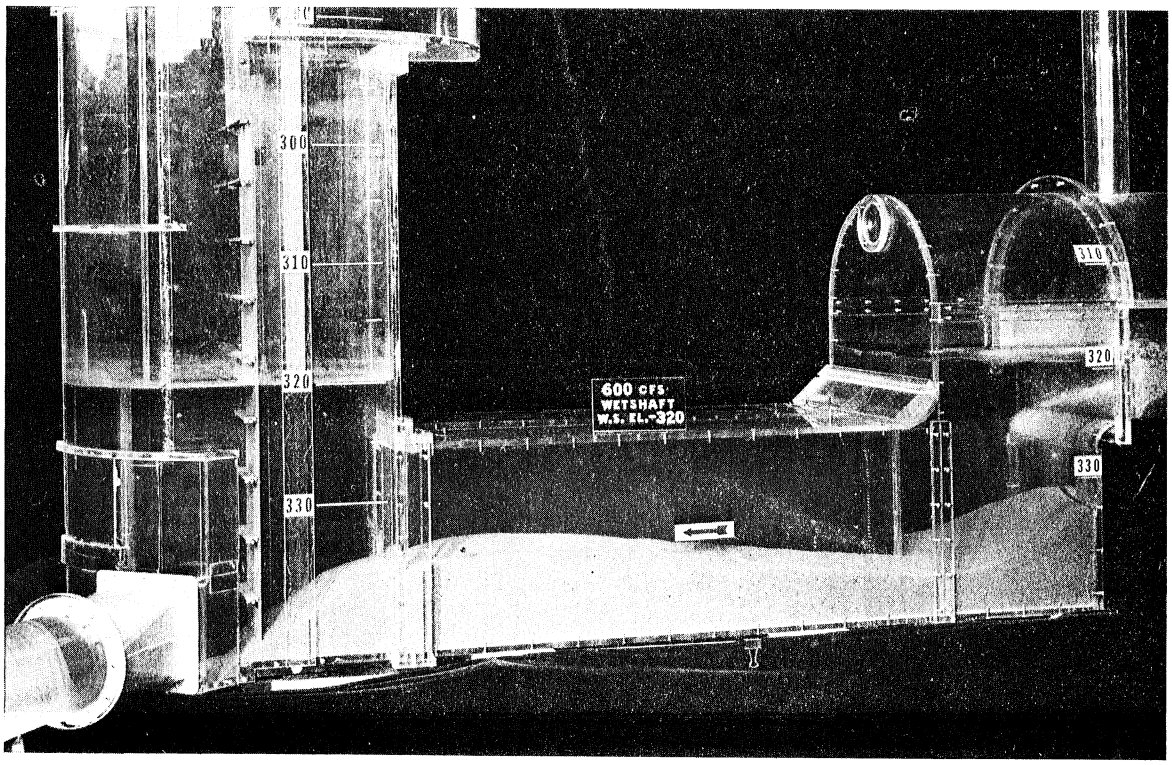

Fig. 53 - Final Stages of Grit Transport through Drop Structure and Divided Duct. Design B.

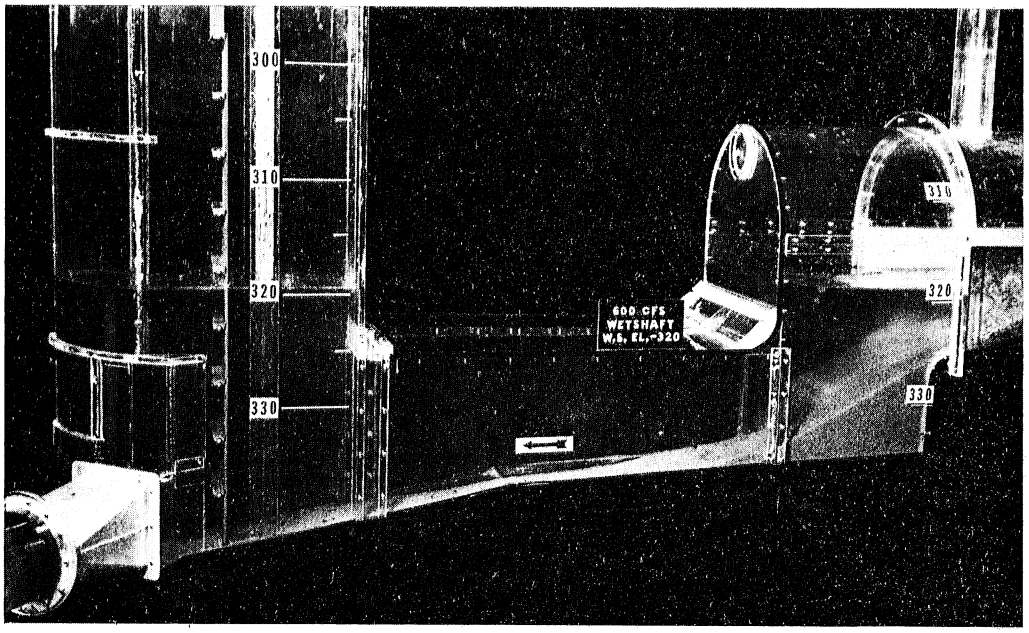

Fig. 54 - Grit Transport. Design C. Approximately 1 Hour Prototype Time Since Sediment Addition.

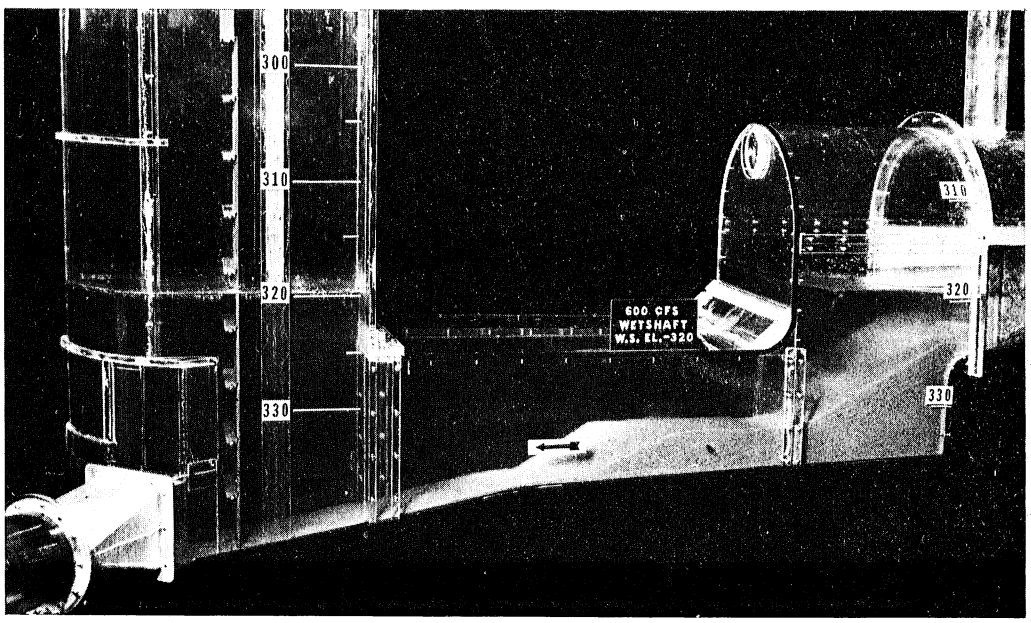

Fig. 55 - Grit Transport. Design C. Approximately 2 Hours Prototype Time Since Sediment Addition. Sediment Feed Stopped.

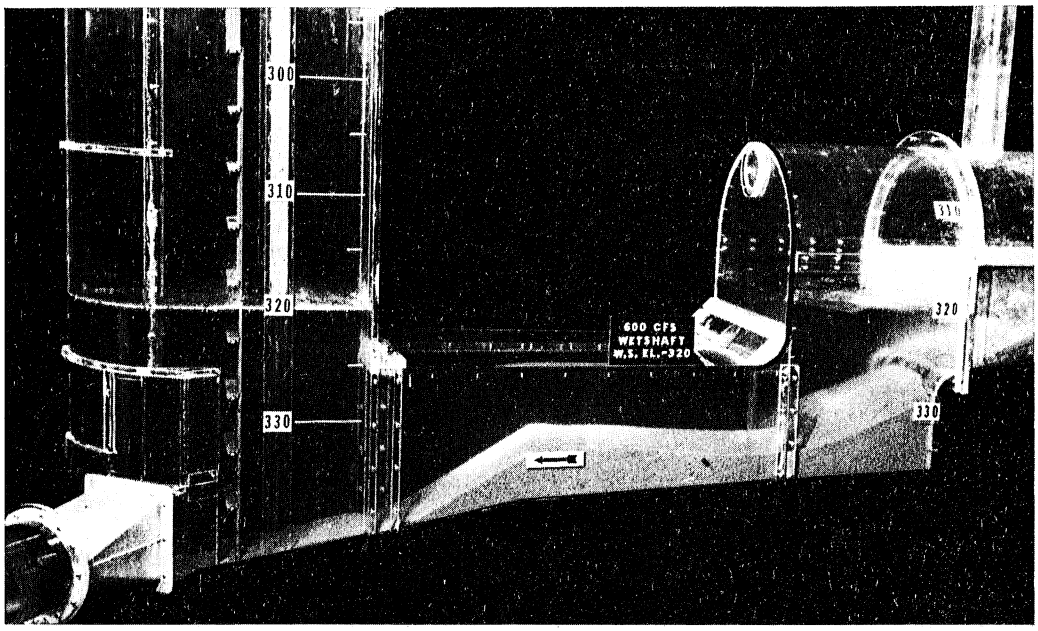

Fig. 56 - Grit Transport. Design C. Approximately 4 Hours Prototype Time Since Sediment Addition.

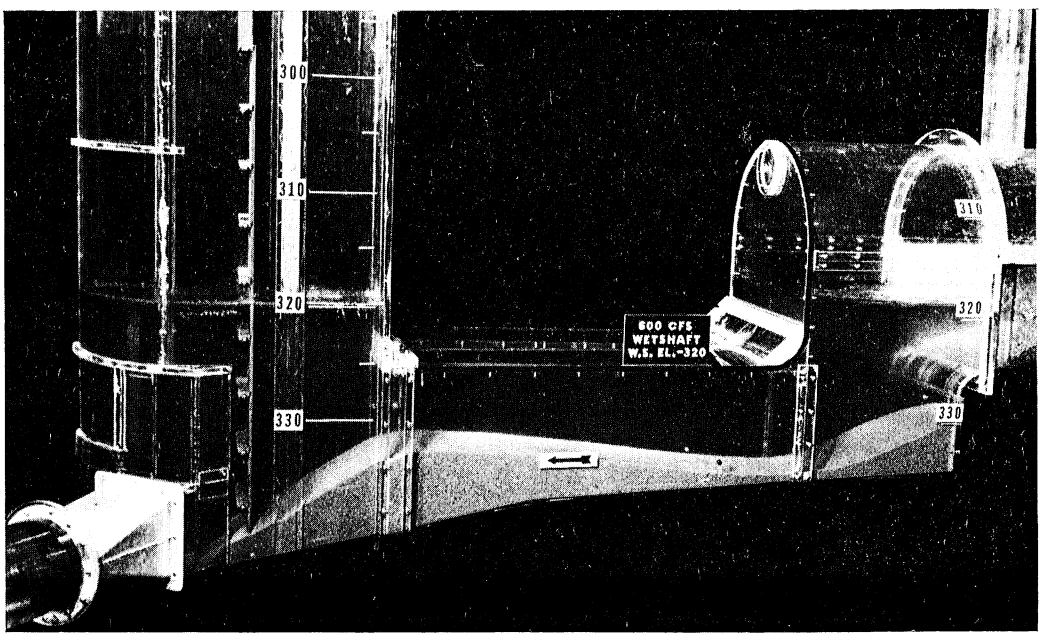

Fig. 57 - Grit Transport. Design C. Approximately 8 Hours Prototype Time Since Sediment Addition.

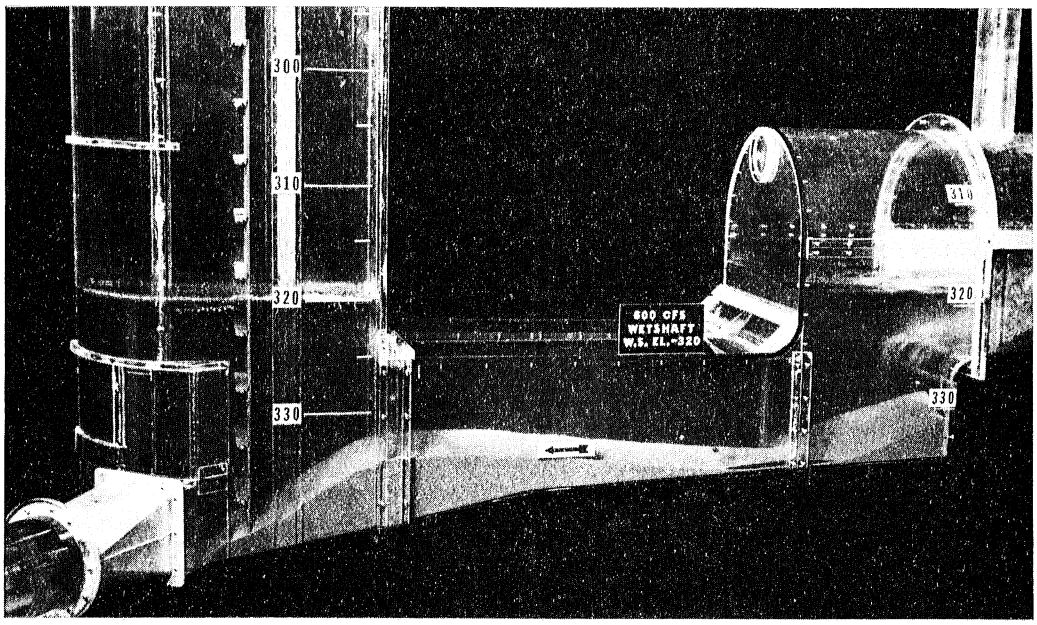

Fig. 58 - Grit Transport. Design C. Approximately 12 Hours Prototype Time Since Sediment Addition.

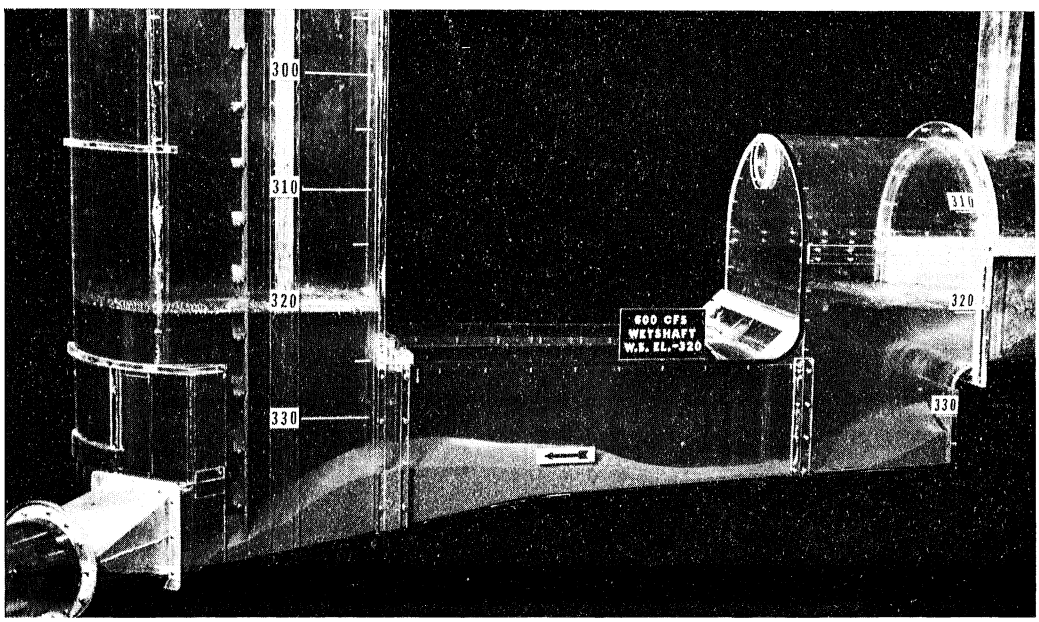

Fig. 59 - Grit Transport. Design C. Approximately 16 Hours Prototype Time Since Sediment Addition.

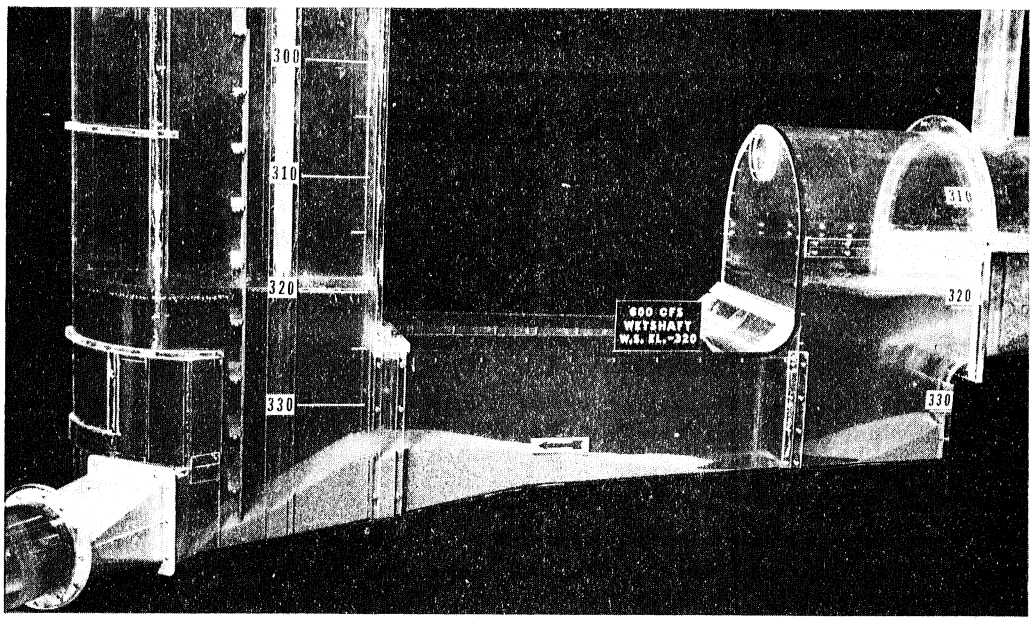

Fig. 60 - Grit Transport. Design C. Approximately 20 Hours Prototype Time Since Sediment Addition.

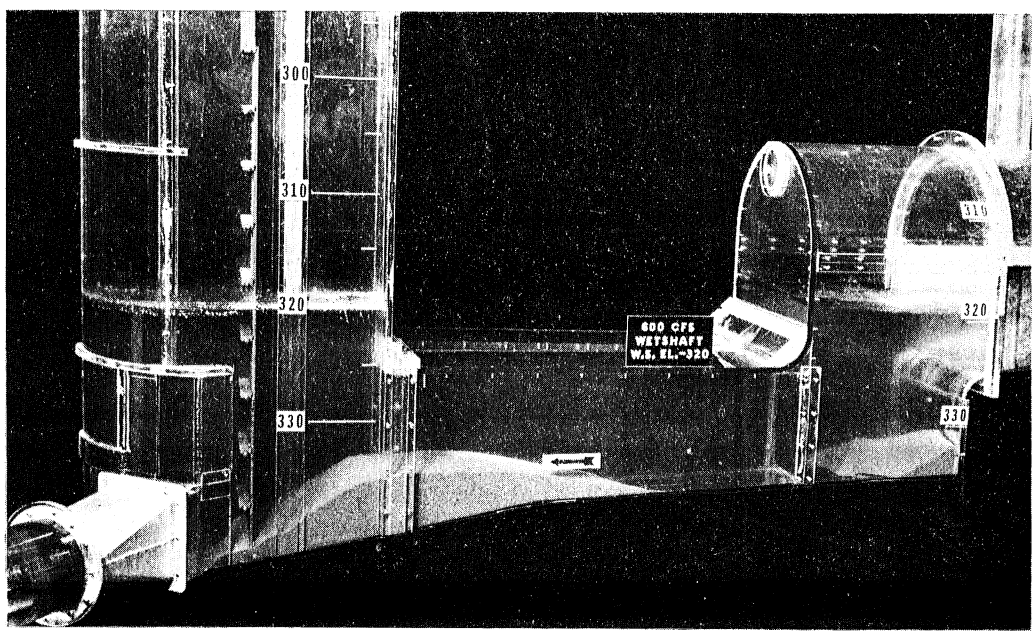

Fig. 61 - Grit Transport. Design C. Approximately 24 Hours Prototype Time Since Sediment Addition.

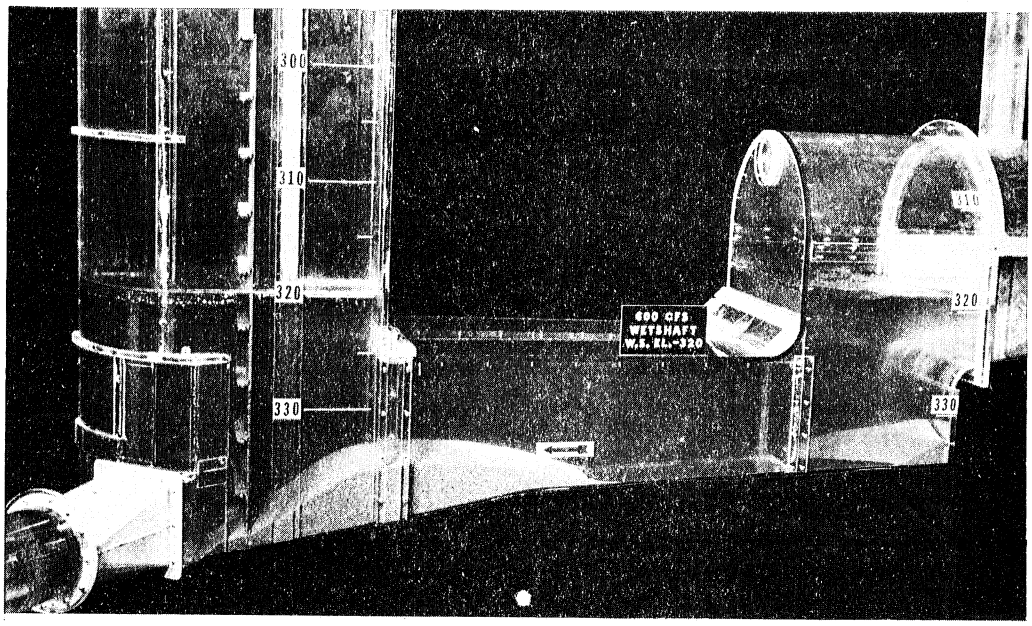

Fig. 62 - Grit Transport. Design C. Approximately 28 Hours Prototype Time Since Sediment Addition.

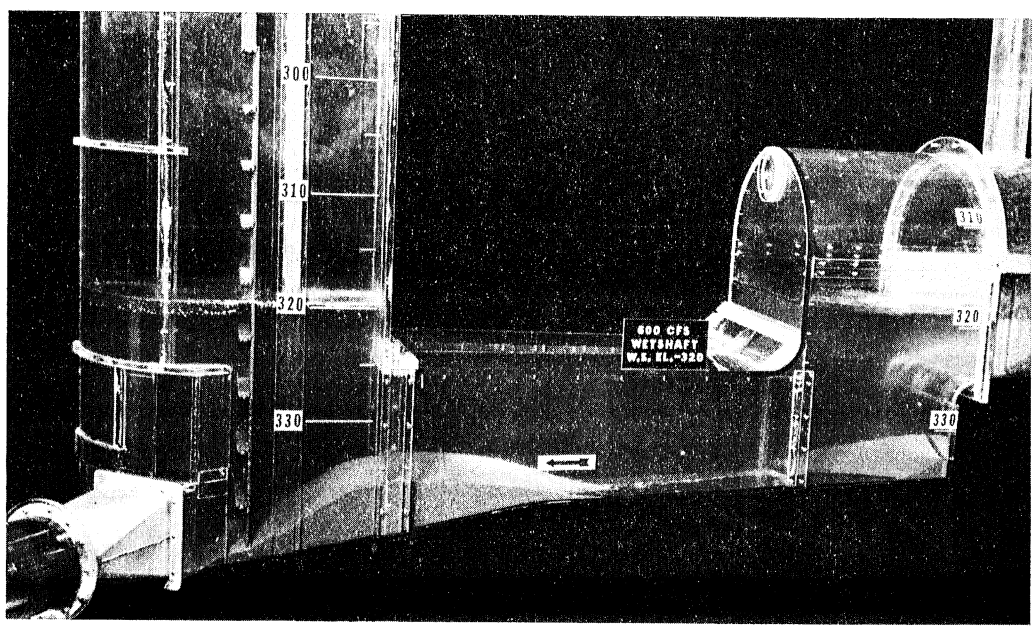

Fig. 63 - Grit Transport. Design C. Approximately 32 Hours Prototype Time Since Sediment Addition.

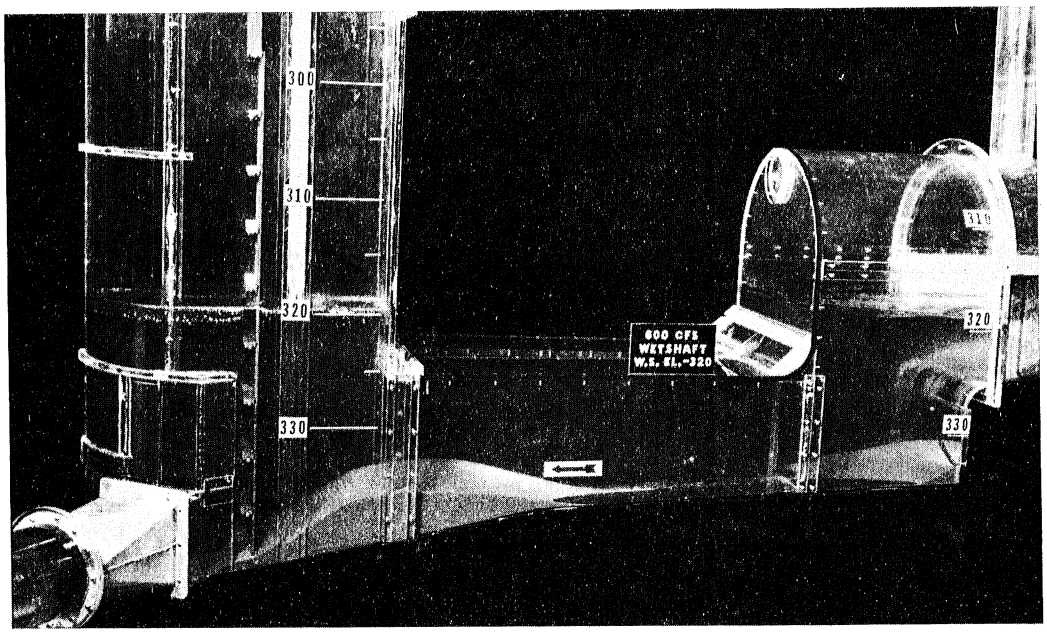

Fig. 64 - Grit Transport. Design C. Approximately 36 Hours Prototype Time Since Sediment Addition.

APPENDIX

Additional Considerations on Similitude

For the study of vortex formation, secondary currents and flow separation in the Calumet intake structure, Froude similarity is an adequate scaling criterion. The presence of a free water surface in the drop structure and in the wet shaft and the frequent change in flow direction and velocity forced upon the water by the geometry of the structure cause a predominance in inertial and gravity effects which are properly modeled by Froude similarity.

Air entrainment from the free surface in the drop structure or in the wet shaft, in addition to density effects, also involves surface tension which is of importance in the break-up of the entrained air into bubbles. Bubble sizes, for example, are therefore not modelled to scale. Scaling according to Weber numbers would be required. Gravitational forces relative to surface tension forces are scaled by the square of the Weber number, which means at a ratio of 1:2744 in this model, assuming that the surface tension and the density of the water in the model and the prototype are the same. The entrainment of air in the drop structure or in the wet shaft of the structure depends for the most part on secondary currents and vortex formation, which are not appreciably affected by surface tension in a model of the size chosen. Observations of air entrainment made in the model will therefore be at least qualitatively similar to those in the prototype.

Entrainment of fuel on the water surface to simulate the results of oil spills depends on buoyant forces, interfacial tension at the water/oil interface and relative viscosity of water and fuel. If model and prototype fuel are the same (kerosene was used in the model) Froude similarity implies that

buoyant forces are scaled properly, i.e. in same proportion as all gravitational forces. Interfacial and viscous forces in the Calumet intake model are minor and not scaled precisely. Model observations on fuel entrainment are therefore qualitative but quite adequate, because the dominant forces are scaled exactly.

Friction head losses due to wall shear stresses in the structure are obviously quite small. In the suction header, model measurements indicate that between Station 3 and Station 9 they are less than 0.1 ft. Since model and prototype are operated at very different Reynolds numbers and have different roughnesses, model measurements of wall friction cannot be transferred directly. Instead, an approximate computational evaluation must be made. Such an evaluation shows that in the prototype at a flow rate of 280 cfs in the suction header, the Darcy friction factor would most likely be near 0.01, resulting in a head loss on the order of 0.2 ft over a length of 210 ft.

Local losses such as at the suction header intake or at the suction header branch points are generally dependent on geometry and to a much smaller degree on Reynolds number. Since geometries in model and prototype are similar, the model should provide representative local losses. Reynolds numbers can be varied in the model to test the sensitivity of the measured loss values but prototype values cannot be attained. The largest suction header Reynolds number attained was 217,000 about one tenth of that in the prototype under full flow. No appreciable, consistent Reynolds number effect was found.

Local head losses across the gate valves (Stations 1-2, 4-5 and 7-8) should not be transferred from the model because the geometries of small and large gate valves are not necessarily geometrically similar. Commercial gate

valves for 3 inch and 2.5 inch pipes were used in the model. Loss coefficients for the 14 times larger prototype units should be obtained from the manufacturer of those units.

Model simulation of grit transport is only qualitative in the model experiment for several reasons. First of all, it is not known what size distribution the prototype grit will have and the model grit is only a geometrical approximation. Second, when Froude similarity is applied, secondary currents and large scale eddies which are important in grit transport are adequately scaled, but exact bed shear stresses which are also important are not. Nevertheless, large numbers of past experiments and comparisons with prototypes show that experiments of the kind performed in the Calumet intake structure give a very good indication of potential local sedimentary problems and their solution.